# Analytical and Experimental Thermal Analysis of a Guided Bomb

W. K. Crain and R. K. Matthews
ARO, Inc.

February 1981

Final Report for Period October 1978 — September 1979

**ARNOLD ENGINEERING DEVELOPMENT CENTER
ARNOLD AIR FORCE STATION, TENNESSEE
AIR FORCE SYSTEMS COMMAND
UNITED STATES AIR FORCE**

This report has been reviewed by the Office of Public Affairs (PA) and is releasable to the National Technical Information Service (NTIS). At NTIS, it will be available to the general public, including foreign nations.

## APPROVAL STATEMENT

This report has been reviewed and approved.

ALVIN R. OBAL, Captain, CF
Project Manager
Directorate of Technology


Approved for publication:

FOR THE COMMANDER

MARION L. LASTER
Director of Technology
Deputy for Operations

# UNCLASSIFIED

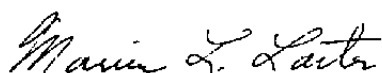| REPORT DOCUMENTATION PAGE | | READ INSTRUCTIONS BEFORE COMPLETING FORM |
|---|---|---|
| 1 REPORT NUMBER<br>AEDC-TR-79-91 | 2 GOVT ACCESSION NO | 3 RECIPIENT'S CATALOG NUMBER |
| 4 TITLE (and Subtitle)<br>ANALYTICAL AND EXPERIMENTAL THERMAL ANALYSIS OF A GUIDED BOMB | | 5 TYPE OF REPORT & PERIOD COVERED<br>Final Report, October 1978 - September 1979 |
| | | 6 PERFORMING ORG REPORT NUMBER |
| 7 AUTHOR(s)<br>W. K. Crain and R. K. Matthews, ARO, Inc., a Sverdrup Corporation Company | | 8 CONTRACT OR GRANT NUMBER(s) |
| 9 PERFORMING ORGANIZATION NAME AND ADDRESS<br>Arnold Engineering Development Center/DOT<br>Air Force Systems Command<br>Arnold Air Force Station, Tennessee 37389 | | 10 PROGRAM ELEMENT PROJECT TASK AREA & WORK UNIT NUMBERS<br>Program Element 62602F |
| 11 CONTROLLING OFFICE NAME AND ADDRESS<br>Arnold Engineering Development Center/DOT<br>Air Force Systems Command<br>Arnold Air Force Station, Tennessee 37389 | | 12 REPORT DATE<br>February 1981 |
| | | 13 NUMBER OF PAGES<br>66 |
| 14 MONITORING AGENCY NAME & ADDRESS(if different from Controlling Office) | | 15 SECURITY CLASS (of this report)<br>UNCLASSIFIED |
| | | 15a DECLASSIFICATION DOWNGRADING SCHEDULE<br>N/A |

16 DISTRIBUTION STATEMENT (of this Report)

Approved for public release; distribution unlimited.

17 DISTRIBUTION STATEMENT (of the abstract entered in Block 20, if different from Report)

19 KEY WORDS (Continue on reverse side if necessary and identify by block number)

| | |
|---|---|
| thermal analysis | stores |
| guided bombs | finite element analysis |
| GBU-8, MK-84 | aerodynamic heating |
| radiant heating | mathematical models |
| test methods | |

20 ABSTRACT (Continue on reverse side if necessary and identify by block number)

As part of a technology program to investigate the transient heating problems associated with high-speed carriage of conventional stores, an analytical and experimental thermal analysis was conducted on a guided bomb. The objective of this work was to investigate the technology necessary to develop an analytic model from which store internal component thermal response could be generated. In addition, a radiant-heat ground test was

DD FORM 1473 1 JAN 73    EDITION OF 1 NOV 65 IS OBSOLETE

## UNCLASSIFIED

20. ABSTRACT (Continued)

conducted on instrumented flight hardware for the purpose of
generating experimental data for calibrating the analytic model.
A new test technique was developed to simulate the predicted
flight heating distribution over the store. The results demon-
strate an analytical and experimental approach for predicting
store internal component thermal response. Comparison of the
analytic model and ground test results shows adequate agreement
in the bomb section but a general lack of agreement in sections
containing electronic components. This lack of agreement is
attributed to the uncertainty in component thermal properties,
contact resistance, modeling assumptions, and general complexity
of the store hardware. The results illustrate the importance in
experimental validation of the analytic model.

AFSC
Arnold AFS Tenn

# PREFACE

# CONTENTS

# ILLUSTRATIONS

## TABLES

# 1.0 INTRODUCTION

## 1.1 BACKGROUND

"In 1970, Hq USAF directed AFSC to establish a program to accomplish two major goals:

(1)    Provide the Air Force with an interim supersonic delivery capability using inventory aircraft and munitions.

(2)    Establish technology programs to solve the technical problems associated with supersonic delivery of conventional ordnance" (Ref. 1).

Some examples of conventional ordnance carried by present-day aircraft are shown in Fig. 1. Included in the photograph are MK-82 and MK-84 iron bombs, GBU-8 guided bombs, munitions dispensers, as well as AIM-9 and AIM-7 guided missiles. Technical problem areas associated with the supersonic delivery of these stores are

a.    Flutter limits for the particular store/aircraft combinations,

b.    Store structural limit,

c.    Fuel consumption during supersonic carriage,

d.    Store/aircraft manueverability, and

e.    Aerodynamic heating of the store and store internal components (Ref. 2).

Because of these problem areas, speed restrictions are placed on the carriage aircraft which limit its full potential. This is illustrated in Fig. 2 which shows the speed capability of several present-day "clean" aircraft and a current speed limitation (700 KCAS*/Mach 1.4 line) imposed with store carriage. In an effort to address these problem areas and close the gap between restricted and clean aircraft limits, the Air Force Armament Laboratory (AFATL)/Arnold Engineering Development Center (AEDC) Store Heating Technology Program was generated. The project is directed toward the transient heating problems associated with high-speed carriage of conventional stores with work directed along two

---

*KCAS - Knots Calibrated Airspeed

5

major lines of effort - (1) the prediction of the external flight heating environment and (2) the response of the store internal components to that environment (see Fig. 3). The desired end result is a technology package which demonstrates the procedures for predicting the thermal response of store internal components to flight conditions.

Within recent years, wind tunnel techniques have been developed to measure the external heating environment on pylon-mounted stores and store internal component thermal response. These techniques, as well as application of wind tunnel results to actual flight conditions, are documented by Matthews et al., in Refs. 3, 4, and 5.

In September 1973, a research project was initiated to investigate the scaling of wind tunnel store external heating measurements to flight conditions. The primary objective of this project was to obtain wind tunnel and flight heating rate measurements on a pylon-mounted store to substantiate the correlation procedure established from theoretical considerations. These procedures are outlined by Matthews et al., in Ref. 6 and Crain and Nutt in Ref. 7. The results of this, and additional work (Refs. 7 through 10), confirmed the application of wind tunnel technology to obtain store heating data for flight conditions. It also demonstrated that "excessive" internal component temperatures can be achieved by store components during high-speed carriage. The results did not, however, conclusively confirm the correlation procedure used to scale the wind tunnel data to flight conditions. Subsequently, the present program was initiated for the purpose of not only verifying the scaling procedure between tunnel and flight but also investigating the technology to analytically predict the response of the store components to the external environment. The program is composed of a coordinated analytic, ground, and flight test effort. The work reported herein deals mainly with the prediction of store internal component thermal response. To date, a particular class of stores has been studied. The studies include the development of a mathematical model and its analytic results to determine the internal component thermal response. In addition, a ground test has been conducted on instrumented flight hardware for the purpose of verifying the mathematical model.

## 1.2 PURPOSE

The purpose of this report is to document the analytic modeling technique, ground test technique, and discuss the agreement between mathematical model and ground test data.

## 2.0 ANALYTIC MODELING

## 2.1 HARDWARE

The store chosen for the thermal response phase of the project was the GBU-8 electro-optical guided bomb (Fig. 4). The store is basically an electro-optical guidance and control

kit fitted around an MK-84 general purpose 2,000-lb bomb. The reason for choosing the GBU-8 is that it represented several areas of interest, i.e., the simpler unguided, unboosted iron bomb category as well as the more complicated electronics component hardware in the guidance and control sections.

## 2.2 STORE MODELING PHILOSOPHY

To assess the effects of aerodynamic heating and predict the thermal response of the store internal components, knowledge of the following is needed:

a.  Definition of flight conditions;

b.  Store external flight heating environment, i.e., flight heating distribution, recovery temperature along the store, and length of time the store is exposed to the environment;

c.  A criterion which will define system failure, i.e., critical components and their temperature limits;

d.  Geometrical description for input to an analytical model and a digital computer code to solve the heat conduction equations; and

e.  Thermophysical properties of the store and store internal components as well as any internal heat generation by the components.

These requirements, as related to the particular store in question, are discussed in the following sections.

### 2.2.1 Flight Conditions

Flight conditions were based on the assumption of a hypothetical cruise-dash mission profile (Fig. 5). This consists of a high-altitude subsonic cruise of sufficient time to establish a relatively consistent equilibrium temperature within the store. The magnitude of this temperature is the store cruise recovery temperature, $T_{r_{cruise}}$. This determines the store initial temperature entering the dash phase ($T_{r_{cruise}} = T_{i_{dash}}$). Delivery of the store is then accomplished by a low-altitude, high-speed dash to the target area where the store temperature increases from the cruise recovery temperature toward the dash recovery temperature.

Limits on parent-aircraft Mach number were assumed to be 0.6 to 1.2 at altitudes of sea level to 40,000 feet. The MIL-STD-210B (Ref. 11) 1 Percent Air Operations Hot and Cold Days was chosen as the altitude-temperature profiles. These climatic extremes are shown in Fig. 6. Temperatures are seen to range from 121°F at sea level to -101°F at 32,800 ft. Over the altitude and Mach number range assumed, the recovery temperature the store would achieve is shown in Fig. 7. Assuming the store has a component which has a maximum temperature limit of 160°F, it is possible to overheat the component at flight conditions as low as Mach 0.6. For critical component temperatures above 160°F, operation within the triangular area of Fig. 7 would be limited in time, i.e., flight time in this area is equal to the time period it takes the critical component to reach its critical temperature.

### 2.2.2 External Flight Heating Environment

The flight heating distribution used for the study is shown in Fig. 8. Corresponding conditions for which it was derived are $M_\infty = 1.2$, sea-level altitude, turbulent boundary layer, and a wall-to-total temperature ratio of 0.90. The distribution includes flow-field interference effects such as carriage on the parent aircraft and proximity to other stores. The interference-free distribution was generated from pressure estimates from the South-Jameson Code (Ref. 12) and turbulent heat-transfer estimates from the BLIMP Code (Ref. 13). The increment attributed to interference effects was taken from experimental data obtained in the Supersonic Wind Tunnel (A) of the AEDC von Kármán Gas Dynamics Facility (VKF), (Ref. 8). This increment is defined as the ratio of heating measured on the store in the aircraft carriage position to the heating measured on the store in the free stream alone. The magnitude of the increment was less than 1.5 over the aft 70 percent of the body, whereas values of 1.4 to 2.0 were applied near the nose.

Recovery temperature distribution along the store was assumed constant. For the purposes of calculation, a value consistent with the equation

$$T_r = T_e\left(1 + 0.2rM_e^2\right) \approx T_\infty\left(1 + 0.18M_\infty^2\right)$$

where

$$r = 0.90 \text{ (Turbulent Recovery Factor)}$$

was chosen. This gives a temperature ratio $T_r/T_0 = 0.98$ or $T_r = 0.98\,T_0$, which is consistent with unpublished experimental data.

From these results, the initial and final temperatures to which the store would be exposed in the dash phase (Fig. 5, Section 2.2.1) are

$$T_{r_{dash}} = T_{\infty_{dash}}\left(1 + 0.18 M^2_{\infty_{dash}}\right)$$

$$T_{i_{dash}} = T_{r_{cruise}} \approx T_{\infty_{cruise}}\left(1 + 0.18 M^2_{\infty_{cruise}}\right)$$

where

$$T_{\infty} = f(altitude), \text{ Fig. 6.}$$

### 2.2.3 Failure Criteria

Unfortunately, no unified criteria for determining system or component failure were available. For this reason, the temperature limits placed on the internal components were obtained from more generalized information and sources. Store critical components, i.e., those adversely affected by the thermal environment, are as follows:

Guidance Section
- Vidicon Assembly
- Electronics Package

MK-84 Bomb Section
- Tritonal Explosive
- Forward and Aft Fuses

Control Section
- Roll Gyro
- Autopilot
- Thermal Batteries
- Signal Inverter

These components and their respective locations in the store are shown in Fig. 4b.

Critical temperatures associated with these components are 178°F for the tritonal explosive in the bomb section and 160°F for the electronics components in the guidance and control sections. The 178°F temperature limit represents that temperature at which the tritonal explosive melts (Ref. 14). The 160°F temperature limit on electronic components was obtained from Ref. 15 and represents the maximum allowable storage temperature. Failure was assumed when the outer layer of tritonal reached 178°F or the case containing the electronics components reached 160°F, whichever occurred first.

The temperature limits are somewhat relative in the heating analysis in that once the thermal response of a particular component is known, the time required to reach a particular temperature limit may be obtained. They are important, however, in that they point out the components which should be considered in the modeling phase.

## 2.2.4 Analytic Model and Heat Conduction Code

The finite element modeling technique (Ref. 16) was used to model the store. A graphic representation of the analytic model and model components is shown in Fig. 9. Areas modeled include the optical dome, stable platform (which contains the vidicon tube and gimbal motors), guidance electronics package, forward fuse, bomb shell, asphalt liner, tritonal explosive, aft fuse, roll gyro, thermal batteries, autopilot and signal inverter, as well as guidance and control fairings and their support bulkheads. Since the store is modeled as an axisymmetric body, only half of the model is shown.

Since electronic component internal properties were not available, only the component cases were modeled and internal heat generation was not accounted for. Those areas internal to the store and bounded by air (such as the roll gyro, thermal batteries, guidance electronics package, etc.) were assumed to be adiabatic boundaries, and heat exchange with the surrounding air was not allowed. Material and material property definitions are given in the following section.

The computer code "TRAX" (Ref. 17) was used to perform the transient heat conduction analysis on the GBU-8 analytic model. The code is a two-dimensional finite element program capable of generating transient or steady-state solutions on axisymmetric or planar bodies. Triangular and quadrilateral bilinear elements are used in the analytic model. Inputs to the program are model geometry, material properties ($\varrho$, $C_p$, and k), boundary conditions of heating distribution (h, Fig. 8), recovery temperature ($T_r$), model initial temperature ($T_i$), and time interval for solution. Provisions for material property variation with time and variable recovery temperature are also included in the program. Solutions are given in the form of node temperature variation with time.

## 2.2.5 Store Component Material and Material Properties

Store component material and material thermophysical properties are listed in Table 1. Component material identification was obtained from general assembly and component drawings generated by North American Rockwell - Columbus Division for the GBU-8 Program. In cases where the material callout was generalized or unidentified, a judgment was made as to material type. Properties consistent with that material were then used in the heat conduction code.

The tritonal explosive in the MK-84 bomb section was replaced with dry plaster so as to render the store inert for the ground test phase. Dry plaster was chosen since it has thermophysical properties similar to those of tritonal.

Material properties were obtained, by and large, from general handbook values and therefore were assumed constant with temperature.* In the case of the asphalt liner in the bomb section and the desiccant in the vidicon tube section of the stable platform, experimental values were obtained from private communications with the manufacturers and the Naval Weapons Center (NWC).

## 2.3 ANALYTIC RESULTS

Using the heating distribution of Fig. 8, an array of computer runs was made covering the full range of flight conditions for the dash phase (triangular area, Fig. 7). Variables for these runs were initial and final temperature, initial temperature being that value of equilibrium temperature achieved during cruise (Fig. 7, below triangular area), and final temperature being the maximum available temperature during dash (Fig. 7, within triangular area). From these runs, comparative responses for the various components were obtained and the most critical component determined. Typical results of the analytic analysis are shown in Fig. 10. The batteries, vidicon tube, and fuses have a relatively low thermal response, whereas the roll gyro, electronics package, and inverter exhibit the highest thermal response. The most critical component is the electronics package in the guidance section.

## 3.0 GROUND TEST

The purpose of the ground test was to generate a set of experimental data on the flight hardware by which the analytic model could be verified. Since the GBU-8 was too large for most supersonic wind tunnels and the heating distribution known a priori, a radiant-heat ground test approach was chosen. In this approach, the test article was supported on a test stand and radiant-heat lamps were used to impose the predicted flight heating distribution on the store. The thermal response of the store internal components was then measured and recorded. In simulating the predicted flight heating distribution, a new test technique based on feedback loop measurements of $\dot{q}$ and $T_w$ was devised. This technique, described in Section 3.3.3, was used to control lamp heat input over the store surface.

---

*Because of the many ways that handbook values of thermophysical properties are stated, a set of conversion constants is presented in Table 2 to aid in converting properties to a common base.

**3.1 APPARATUS** limits are somewhat relative in the heating analysis in that once the thermal response of a particular component is known, the time required to reach a particular

**3.1.1 Radiant Heat Test Stand** ed. They are important, however, in that they point out the components which should be considered in the modeling phase.

The test stand consisted of a test article/lamp support chamber and external shroud (Fig. 11). The test article/lamp support chamber was made up of a cylindrical steel frame mounted to a circular steel support plate. The frame supported a copper busswork externally and lamp reflectors and holders internally. Internal dimensions of the chamber were 26 in. ID by 56 in. high (Fig. 12). The test article was lowered into the chamber by an overhead crane and rested on the circular support plate during testing. The top 50 in. of the inside of the chamber were lined with 322 1-kw Quartz-Line® lamps (Model Q1000 T3/4CL). These lamps were arranged in 46 cylindrical rows with seven lamps per row and mounted such that the lamp axis was in the horizontal plane for maximum lamp life (Fig. 13). e is modeled as an axisymmetric body, only half of the model is shown.

For test requirements below ambient temperature, the chamber was covered by a removable insulated shroud (Fig. 11). The shroud wall was 2 in. thick and made of fiberglass sandwiched between an internal and external aluminum shell. The shroud was lowered in place by use of an overhead crane. Liquid (LN₂) and gaseous (GN₂) nitrogen were used to cool the shroud wall and test article. The shroud contained cooling passages for LN₂ hookup. In addition, provisions were available whereby GN₂ could flow directly onto the test article without having to circulate around the shroud wall.

**3.1.2 Electrical Design** e "TRAX" (Ref. 17) was used to perform the transient heat conduction analysis on the GBU-8 analytic model. The code is a two-dimensional finite cle Power to the lamps was supplied by 24 15-kw variable voltage supplies, one for each of the 24 heater circuits. Each circuit could be manually operated by the individual circuit control amplifiers. These were used for heater checkout, calibration, and to set the axial heating distribution on the model. Since lamps on the same cylindrical row were connected to form a circuit, the axial heating distribution could be set by adjusting the individual circuit controllers to different voltage levels relative to each other. During a typical test run, the individual controllers were slaved to a variable power supply which then provided overall lamp voltage control. An electrical schematic is shown in Fig. 14.

2.2.5 Store Component Material and Material Properties

**3.1.3 Test Article**

Store component material and material thermophysical properties are listed in Table 1. Cor The test article was the GBU-8 electro-optical guided bomb previously described in Section 2. and shown in Fig. 4. Actual flight hardware was used for the test. In order to conserve fabrication costs and electrical power, the store was divided into three sections — guidance, bomb, and control — and tested in parts. The bomb section was composed of a heat conduction code.

40-in. section removed from the MK-84. Dry plaster was used as a filler since it had thermal properties similar to the tritonal explosive. To increase the radiant energy absorptance, the test articles were painted with a light coat of high-temperature flat black paint. The disassembled test hardware is shown in Fig. 15.

### 3.1.4 Installation

The three test articles were installed in the test chamber by overhead crane. Each article was centered radially in the chamber and height adjustment was made with firebricks. An installation photograph of the guidance section is shown in Fig. 16. The picture was taken with the lamps at 40 percent of full power.

### 3.2 INSTRUMENTATION

Store instrumentation consisted of Gardon thermopile heat-transfer-rate gages for measuring surface heat flux and store wall temperature. Gage description and operation are described in Ref. 18. Internal component temperatures were measured using Chromel[®]-Alumel[®] thermocouples referenced to a 150°F reference junction.

Gardon gage locations for the MK-84 bomb section are shown in Fig. 17. In addition, the bomb contained two thermocouple-instrumented rakes used to provide radial temperature measurements from the asphalt liner/plaster interface inward (Fig. 18). The rakes were placed so that the thermocouples were at the same axial station as the Gardon gages but rotated ≈ 10 deg radially with respect to the gages. Rake thermocouple locations are given in Table 3.

Gardon gage locations for the guidance and control sections are shown in Figs. 19 and 20, respectively. Internal component thermocouple instrumentation for the the guidance section is shown in Fig. 21. Stable platform, vidicon drive motor, and vidicon tube (Fig. 21a) as well as the guidance electronics package (Fig. 21b) were instrumented. Components in the guidance electronics package containing thermocouples were the exterior case and one printed circuit card. In addition, electronic components at the base of the package were instrumented. Thermocouple instrumentation for the control section is shown in Fig. 22. Batteries, battery support tray, autopilot, and power inverter (Fig. 22a) were instrumented as well as the roll gyro and external case (Fig. 22b). Internal component thermocouples were attached with conductive epoxy or small screws.

## 3.3 TEST DESCRIPTION

### 3.3.1 Test Phases

The test was conducted in two phases. The first (Phase A) was concerned with determining which section — guidance, control, or bomb — had the most critical component.* For this phase, one specific test condition was applied to all three sections and a selection of the most critical section/component made. For the second part of the test (Phase B), the most critical section was placed in the test chamber and an expanded test matrix run in order to obtain internal component thermal response data. Store electronic systems were not powered; therefore, internal component heat generation was not taken into account. This assumption is acceptable in terms of the present project but could not be applied in store development work.

### 3.3.2 Test Conditions

The test conditions consisted of the GBU-8 predicted flight heating distribution (Fig. 8) as well as initial and recovery temperatures corresponding to the mathematical model runs. As previously stated in Section 2.2.2,

$$T_{r_{dash}} \approx T_{\infty_{dash}}\left(1 - 0.18 M^2_{\infty_{dash}}\right) \text{ (Fig. 7)}$$

$$T_{i_{dash}} = T_{r_{cruise}} \approx T_{\infty_{cruise}}\left(1 + 0.18 M^2_{\infty_{cruise}}\right) \text{(Fig. 7)}$$

$$T_{\infty} = f(\text{altitude}) \text{ (Fig. 6)}$$

Thus, the test conditions were connected to the hypothetical mission depicted in Fig. 5. The turbulent heating distribution used in the ground tests (taken from Fig. 8) was assumed constant over the section of store length tested. For the Phase A tests, values of heat-transfer coefficients applied to the three store sections are (from Fig. 8)

---

*The most critical component is that component which reaches its critical temperature first.

| Section | $h(Btu/ft^2-sec-°F)$ | Span of Test Article, in., Fig. 8 |
|---------|----------------------|-----------------------------------|
| Guidance | 0.044 | 0 to 45 |
| Bomb | 0.032 | 70 to 108 |
| Control | 0.028 | 108 to 148 |

Initial and final temperatures were chosen such that the difference between the two (driving potential, $T_r - T_i$) was constant at 170°F. For Phase B, a constant axial heating distribution was used (h = 0.032 Btu/ft²-sec-°F) with values of driving potential ranging from 20 to 250°F.

### 3.3.3 Flight Heating Simulation Philosophy

The objective of the flight heating simulation was to maintain a constant h over the surface of the store (Fig. 8). To do this, a feedback loop was devised based on measurements of $\dot{q}$ and $T_w$. Since $h = \dot{q}/(T_r - T_w)$ and $T_r$ is a fixed value, $\dot{q}$ is a maximum at $T_w = T_i$. The heating rate then decreases proportionately as $T_w$ increases. The philosophy of this technique is depicted in Fig. 23. Predicted flight heating inputs $(h, T_r)$ are loaded into the computer. The store is cooled to a desired $T_i$, and lamp voltage is set to a value estimated to give $\dot{q}_{initial} = h (T_r - T_i)$. The lamps are then turned on instantaneously to simulate a step input in heating consistent with the mathematical model. From the resulting heating rate and wall temperature measurements obtained from the control Gardon gage, an effective heat-transfer coefficient is calculated. The calculated h and desired h are then compared and an error signal generated and displayed on the light panel in the form of percent above or below the desired h. An operator monitors the error signal display and manually adjusts the lamp voltage controller such that a null or near-to-null display is maintained. Control on heat-transfer coefficient is maintained until the wall temperature reaches a value within approximately 5 deg of $T_r$. At this point, the lamp voltage is controlled such that wall temperature does not exceed $T_r$. The store wall temperature is maintained at $T_r$ for 20 to 30 min to allow the internal components to soak in the $T_r$ environment. The ability to maintain a constant h over the surface of the store centers in being able to simultaneously measure and control the incident heat flux and associated wall temperature rise with time.

## 3.4 TEST RESULTS

### 3.4.1 Flight Heating Simulation and Lamp Control

The heating control philosophy outlined in Section 3.3.3 worked very well on constant wall thickness sections such as the MK-84 bomb. However, on sections with variable wall

thickness, such as the guidance and control sections, a different philosophy had to be adopted. This was attributed to the fact that lamp control was relegated to a single Gardon gage. Controlling on gages in the thicker walled sections resulted in gross temperature overshoots in the thin-walled sections. This is illustrated in Fig. 24 which is a plot of wall temperature versus time for the guidance section. On very thin-walled sections, such as the guidance section dome, wall thermal response was so fast that control had to be based on $T_w$ alone. Consequently, several runs were required on each section with variable wall thickness in order to determine the best gage to use for control. This illustrated the need for segmented axial heating distribution control for tests on articles of variable wall thickness. The technique was successful, and the results demonstrate the capability to perform this type of testing in which high heating rates and high lamp densities are required at atmospheric conditions.

### 3.4.2 Radiant-Heat Chamber Performance

Spatial uniformity of $\dot{q}$ and $T_w$ within the test cell is given in Fig. 25. The measurements are from the two rings of instrumentation on the bomb section (Fig. 17), thereby giving a circumferential sample near the top and bottom of the test cell. The top ring was located 30 in. above the test cell floor and the bottom ring 20 in. above the floor. The distributions are normalized with respect to the control Gardon gage. The $\dot{q}$ is uniform within ±8 percent and the $T_w$ distribution within ±6 percent, or ±10°F.

Accuracies of the heating rate and $T_w$ measurements are estimated to be ±7 percent of reading and ±5°F, respectively.

### 3.4.3 GBU-8 Thermal Response

Results of the GBU-8 ground test are presented in Figs. 26, 27, and 28 for the guidance, bomb, and control sections, respectively. Input heat flux and internal component temperature are plotted versus time. To remove the effect of initial and final temperature variations between runs and place the data on a comparative basis, the results are presented in the form of a nondimensional thermal response parameter, $\bar{T}$ (Fig. 29). These experimental results show the bomb section as containing the most critical component (Fig. 29b), with the asphalt/plaster interface reaching its critical temperature in 7.5 min elapsed time. The plaster layer, 0.25 in. into the bomb, reached its critical temperature in 25 min elapsed time. Other components in descending order of thermal response are the electronics case (Fig. 29a) and power inverter (Fig. 29c), with corresponding times to critical temperature of 33 and 48 min. By comparison the vidicon tube, autopilot, and thermal batteries have lower thermal responses. A summary of components and their time to critical

temperature is presented in Table 4. Bomb section circumferential thermal response is shown in Fig. 30. Temperature measurements at the asphalt/plaster interface, also 0.50 in. into the plaster, are presented. Differences up to 40°F in interface temperature are noted at the three circumferential locations. This variation is attributed to a nonuniform circumferential variation in thickness of the asphalt liner. Posttest measurements of the liner thickness showed variations from 0.10 to 0.20 in.

## 4.0 ANALYTIC MODEL/GROUND TEST AGREEMENT

The comparison of the mathematical model and the ground test results is summarized in Fig. 31. Nondimensional thermal response ($\overline{T}$) versus time for components in the guidance (Fig. 31a), bomb (Fig. 31b), and control (Fig. 31c) sections is presented. The best agreement is exhibited in the bomb section (Fig. 31b) where the geometry is axisymmetric. A comparison of the mathematical model and ground test data for the guidance and control sections (Figs. 31a and c, respectively) exhibits a general lack of agreement. In these areas, the mathematical model was approximate because of the lack of definition of the internal parts. The large disparities between the ground test and the analytic results in these sections are attributed to uncertainty in thermal properties, component contact resistance, axisymmetric modeling assumptions, and general complexity of the store hardware. The comparative results point out the need for ground tests to verify analytic results, especially in areas where there is a high degree of mechanical and thermal complexity. The ground test results provide a basis for testing some of the assumptions inherent in the mathematical modeling. In addition, the comparisons indicate that considerable detail must be applied in ascertaining actual hardware geometry as well as thermal and mechanical properties if accurate results are to be obtained.

## 5.0 CONCLUSIONS

As part of a technology program to investigate the transient heating problems associated with high-speed carriage of conventional stores, an analytical and experimental thermal analysis was conducted on a guided bomb. Specific conclusions are as follows:

1.  The results demonstrate an analytical and experimental approach for predicting the thermal response of store internal components.

2.  The radiant-heat ground test technique proved to be a viable tool in obtaining internal component thermal response.

3.   A comparison of the analytic model and ground test results shows adaquate agreement in the bomb section but a general lack of agreement in the sections containing electronic components. This lack of agreement is attributed to the uncertainty in component thermal properties, contact resistance, axisymmetric modeling assumption, and the general complexity of the store hardware. This lack of agreement illustrates the importance of experimental validations of analytic results.

## REFERENCES

1.  Hume, Robert A., Jr. "Supersonic Delivery of Selected Conventional Munitions from F-4 and F-111 Aircraft." AFATL-TR-75-69, May 1975.

2.  Epstein, Charles S. "Supersonic Delivery of Conventional Weapons - Fact or Fancy?" Aircraft/Stores Compatibility Symposium, AFFDL-TR-72-67, Vol. 1, August 1972, pp. 51-72.

3.  Baker, S. S. and Matthews, R. K. "Demonstration of the Thermographic Phosphor Heat-Transfer Technique as Applied to Aerodynamic Heating of External Stores." AEDC-TR-73-128 (AFATL-TR-73-154) (AD769306), November 1973.

4.  Matthews, R. K. and Hube, F. K. "Thermal Response Tests of the FMU-110/B and FMU-113/B Fuses." AEDC-TR-75-120 (AFATL-TR-75-121), October 1975.

5.  Matthews, R. K., Baker, S. S., and Key, J. C., Jr. "Wind Tunnel Heating Test of Aircraft Stores." Aircraft/Stores Compatibility Symposium Proceedings, JTCG/ALNNO WP-12-2, Vol. 4, September 1973.

6.  Matthews, R. K. and Key, J. C., Jr. "Flight Test Heat-Transfer Measurements on a Pylon-Mounted Store." Aircraft/Stores Compatibility Symposium Proceedings, JTCG/MD WP-12, Vol. 2, September 1975.

7.  Crain, W. K. and Nutt, K. W. "Extrapolation of Wind Tunnel Heating Data on a Supersonic Tactical Missile (STM) to Flight Conditions." AEDC-TR-79-30, September 1979.

8.  Matthews, R. K., Spencer, G. D., and Key, J. C., Jr. "Pressure and Heat-Transfer Measurements on Several Pylon-Mounted Store Configurations." Aircraft/Store Compatibility Symposium, JTCG/MD WP-12, Vol. 2, October 1977.

9. Matthews, R. K., Tolley, H. D., and Nutt, K. W. "A Stand-Alone Airborne Data Recording System." Paper Presented at 1978 Air Data Systems Conference, USAF Academy, May 1978.

10. Matthews, R. K. "A Summary Report on Store Heating Technology." AEDC-TR-78-46 (ADA059415), September 1978.

11. Department of Defense. "Military Standard Climatic Extremes for Military Equipment." MIL-STD-210B. December 15, 1973.

12. Yaros, Steven F. "An Analysis of Transonic Viscous/Inviscid Interactions on Axisymmetric Bodies with Solid or Real Plumes." AEDC-TR-77-106 (ADA050401), February 1978.

13. Edenfield, E. E. "Applications of the Aerotherm BLIMP Boundary-Layer Program to Nonablating Reentry Flight Conditions." AEDC-TR-79-6 (ADA071353), July 1979.

14. Departments of the Army and Air Force "Military Explosives." TM9-1300-214, November 1967.

15. ADTC/Eglin AFB/340 "Storage and Maintenance Procedures with Illustrated Parts Breakdown for Bomb Guidance Kits KMU-353A/B and KMU-390/B." T.O. 11K1-47, August 15, 1975.

16. Huebner, Kenneth, H. *The Finite Element Method for Engineers.* John Wiley – Interscience, New York, 1975.

17. Rochelle, James Kenneth. "TRAX–A Finite Element Computer Program for Transient Heat Conduction Analysis of Axisymmetric Bodies." Master's Thesis, University of Tennessee Space Institute, June 1973.

18. Trimmer, L. L., Matthews, R. K., and Buchanan, T. D. "Measurement of Aerodynamic Heat Rates at the AEDC von Kármán Facility." International Congress on Instrumentation in Aerospace Simulation Facilities, IEEE Publication CHO 784-9 AES, September 1973.

Photograph Courtesy of
McDonnell Douglas -
St. Louis

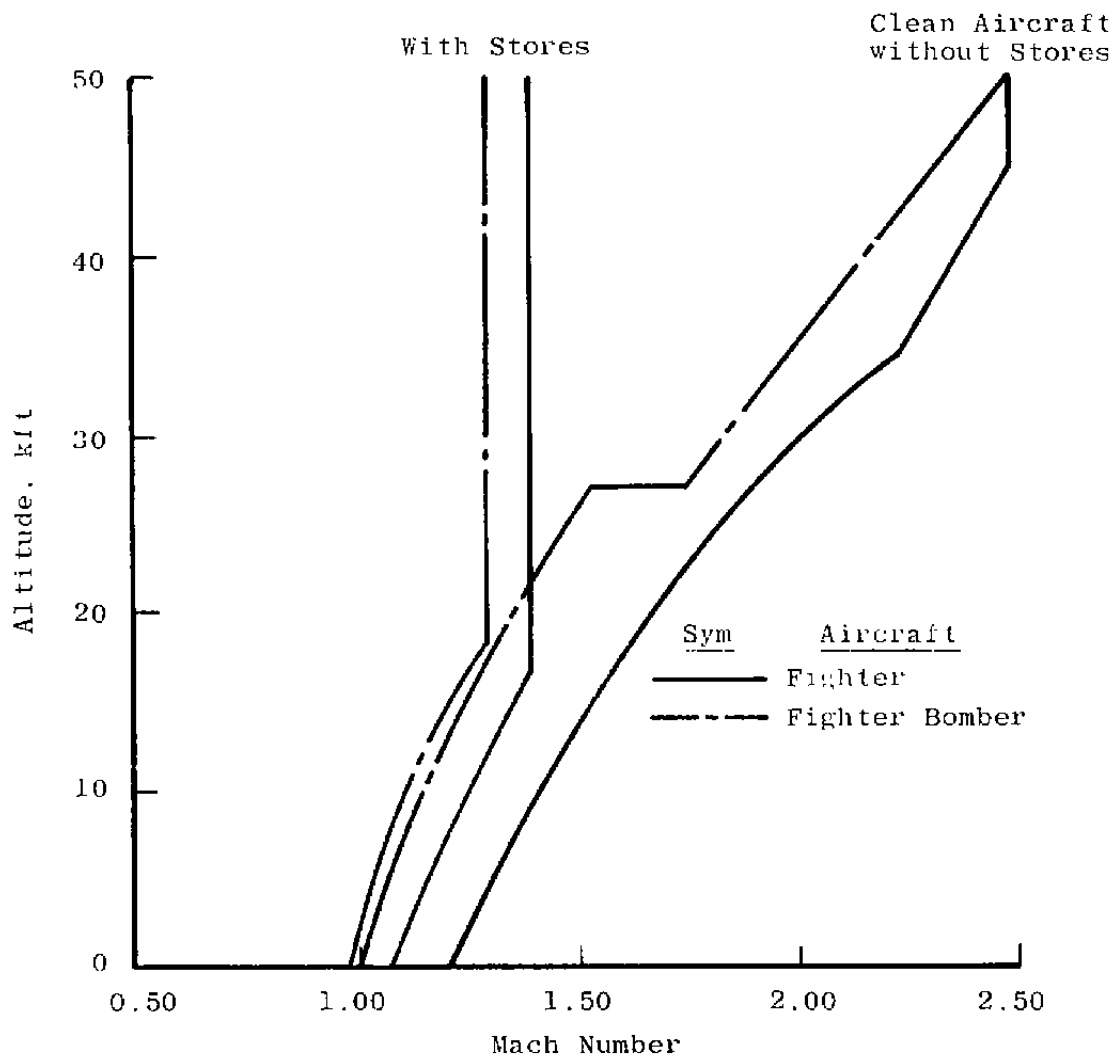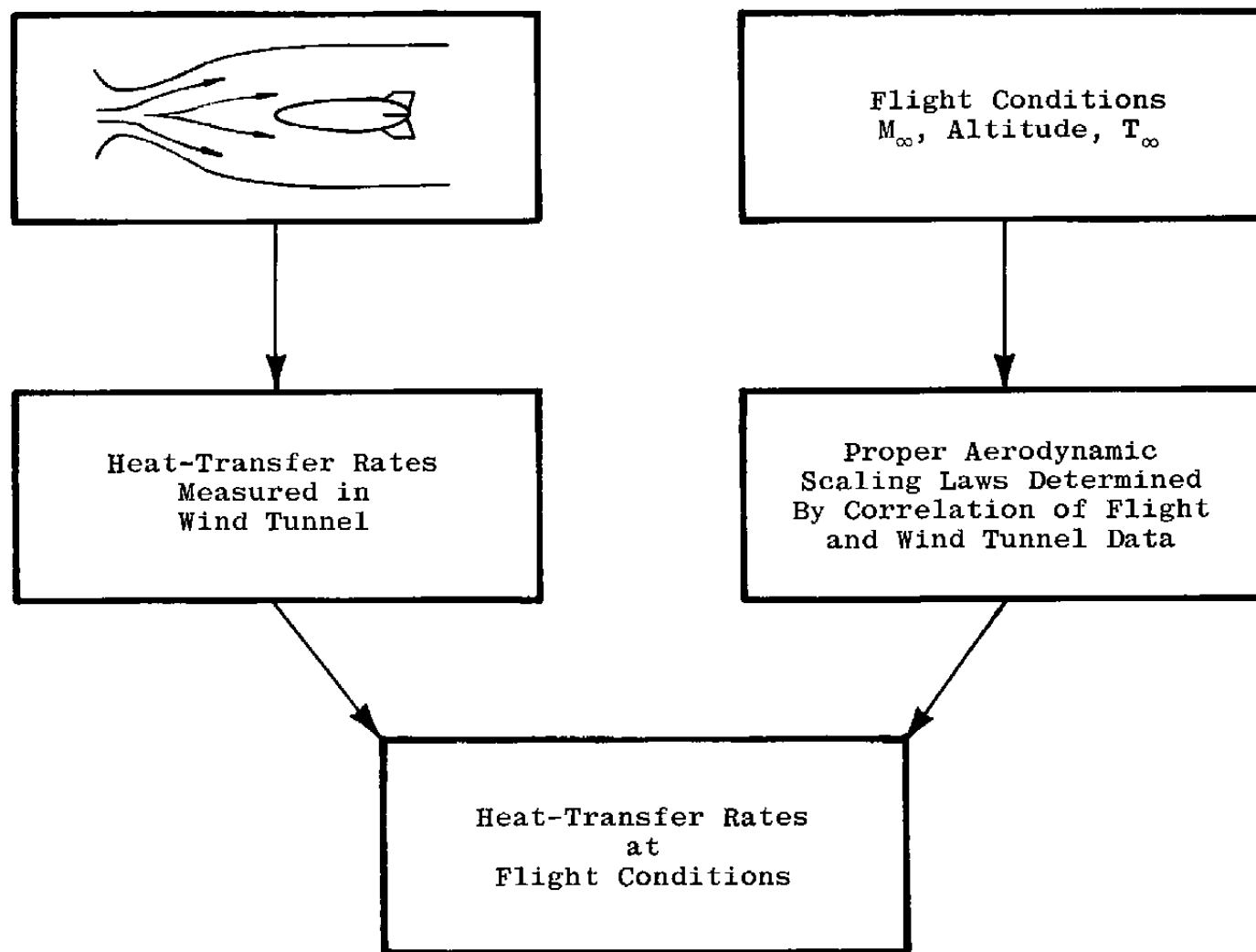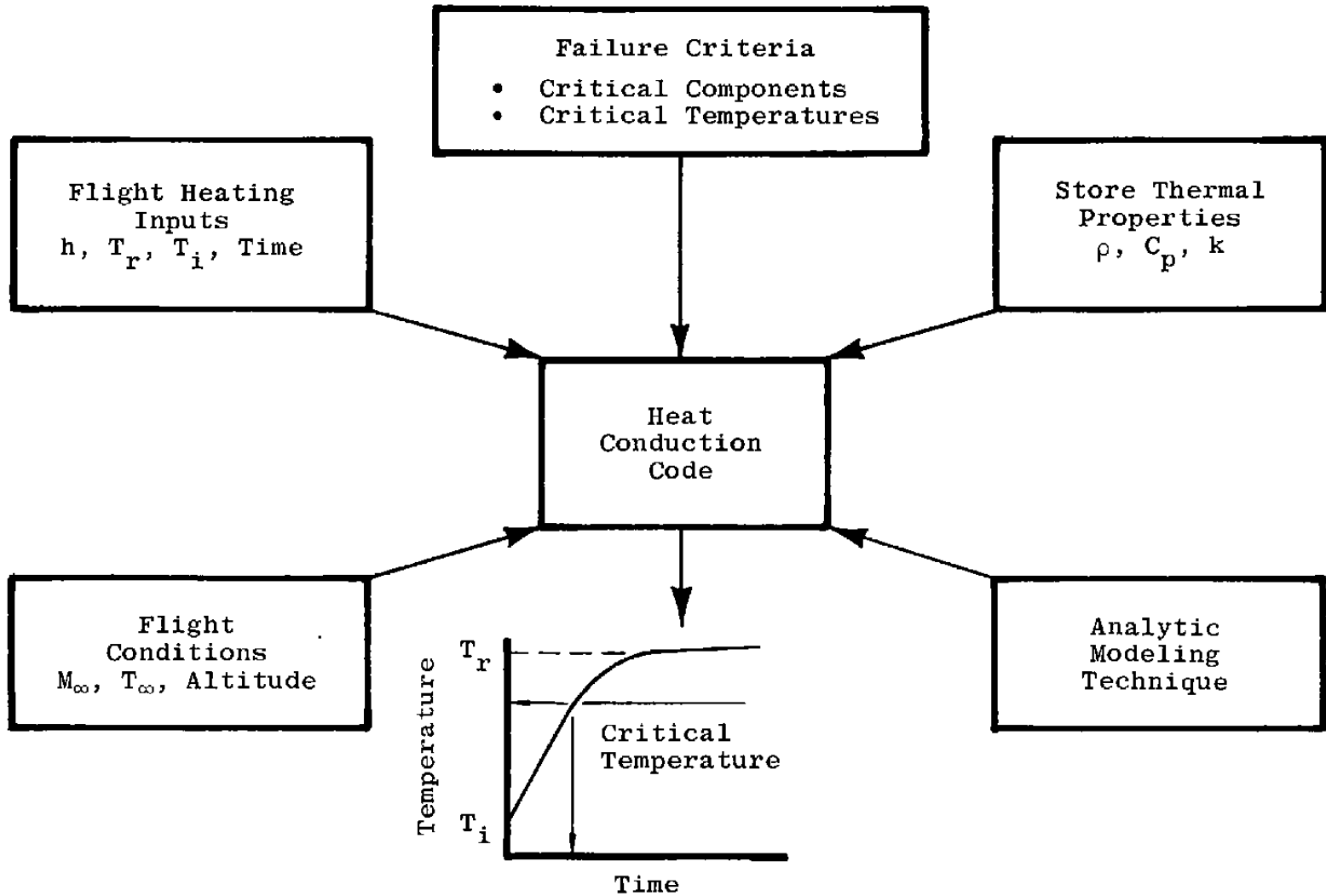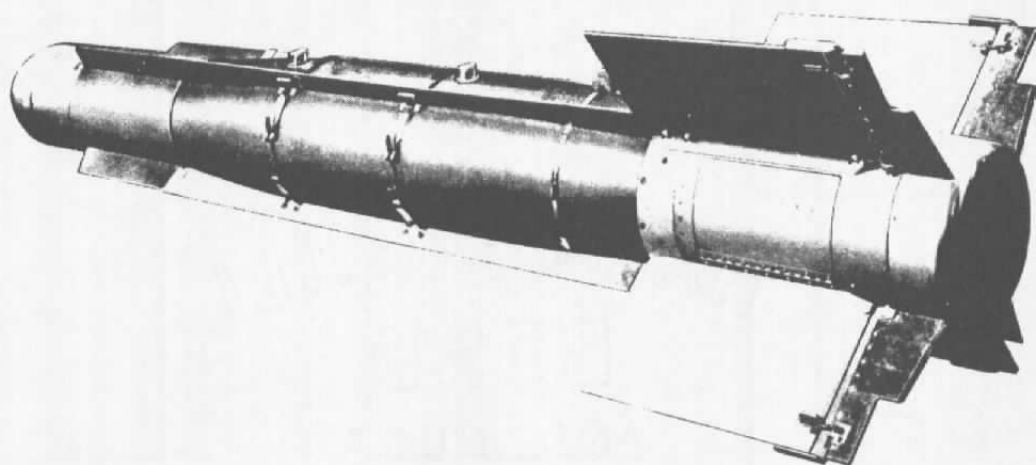Figure 1.  Present-day fighter showing conventional ordnance.

Figure 2. Aircraft and weapons airspeed restrictions.

a. Prediction of store external flight heating environment
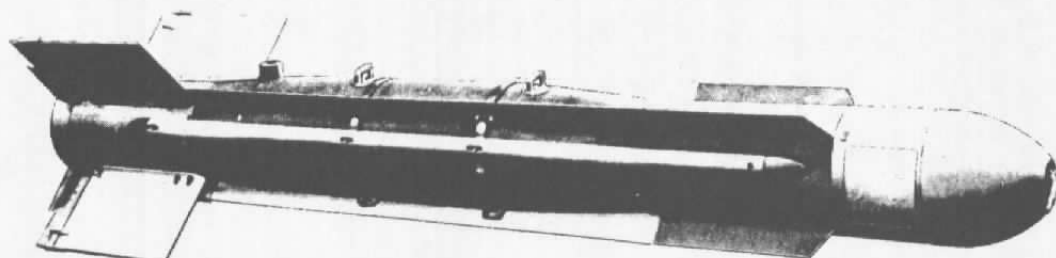Figure 3. Work areas addressed by project.

b. Store internal component thermal response
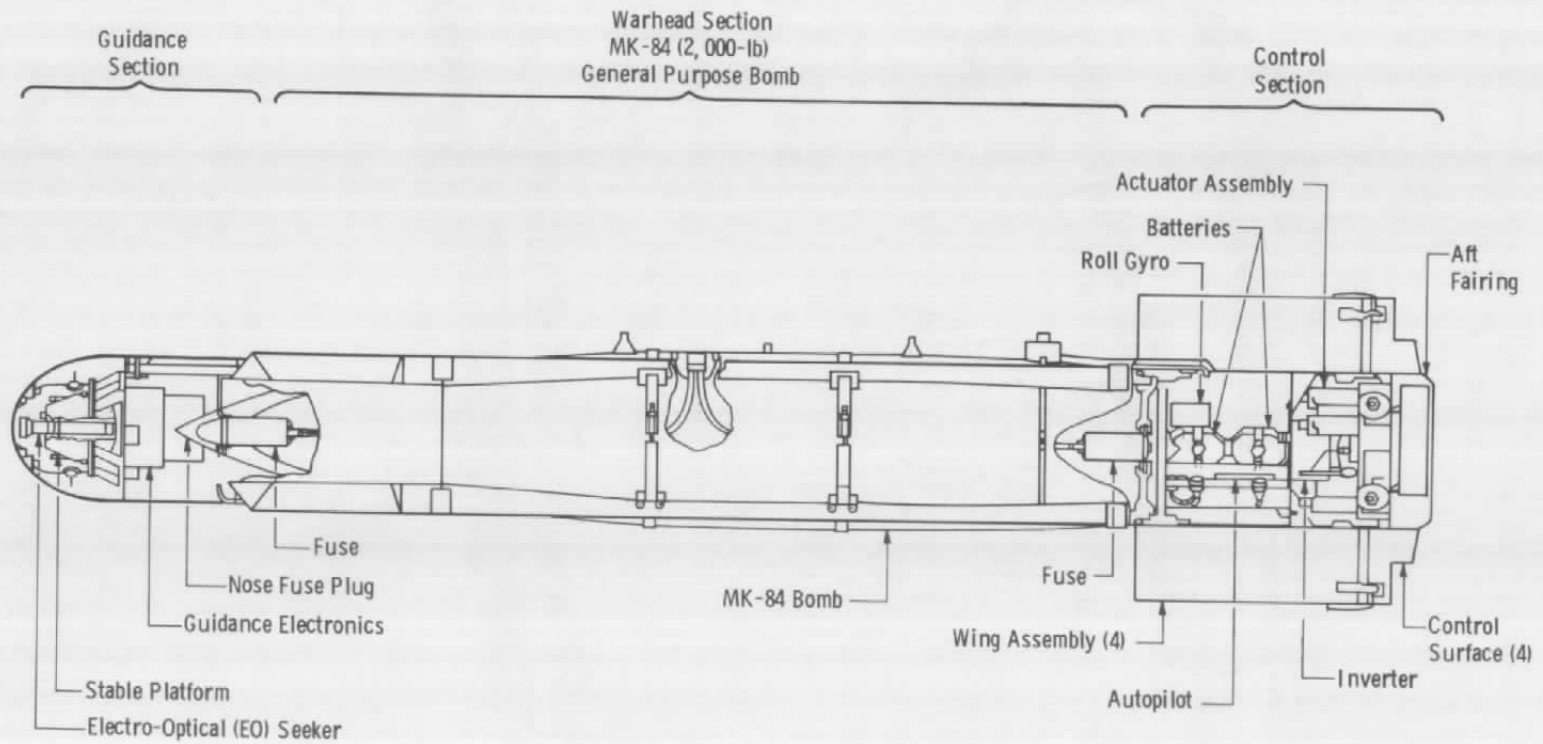Figure 3. Concluded.

Control Section          MK-84 Bomb          Guidance Section



a. External features
Figure 4.  GBU-8 electro-optical guided bomb.

b. Internal component arrangement
Figure 4. Concluded.
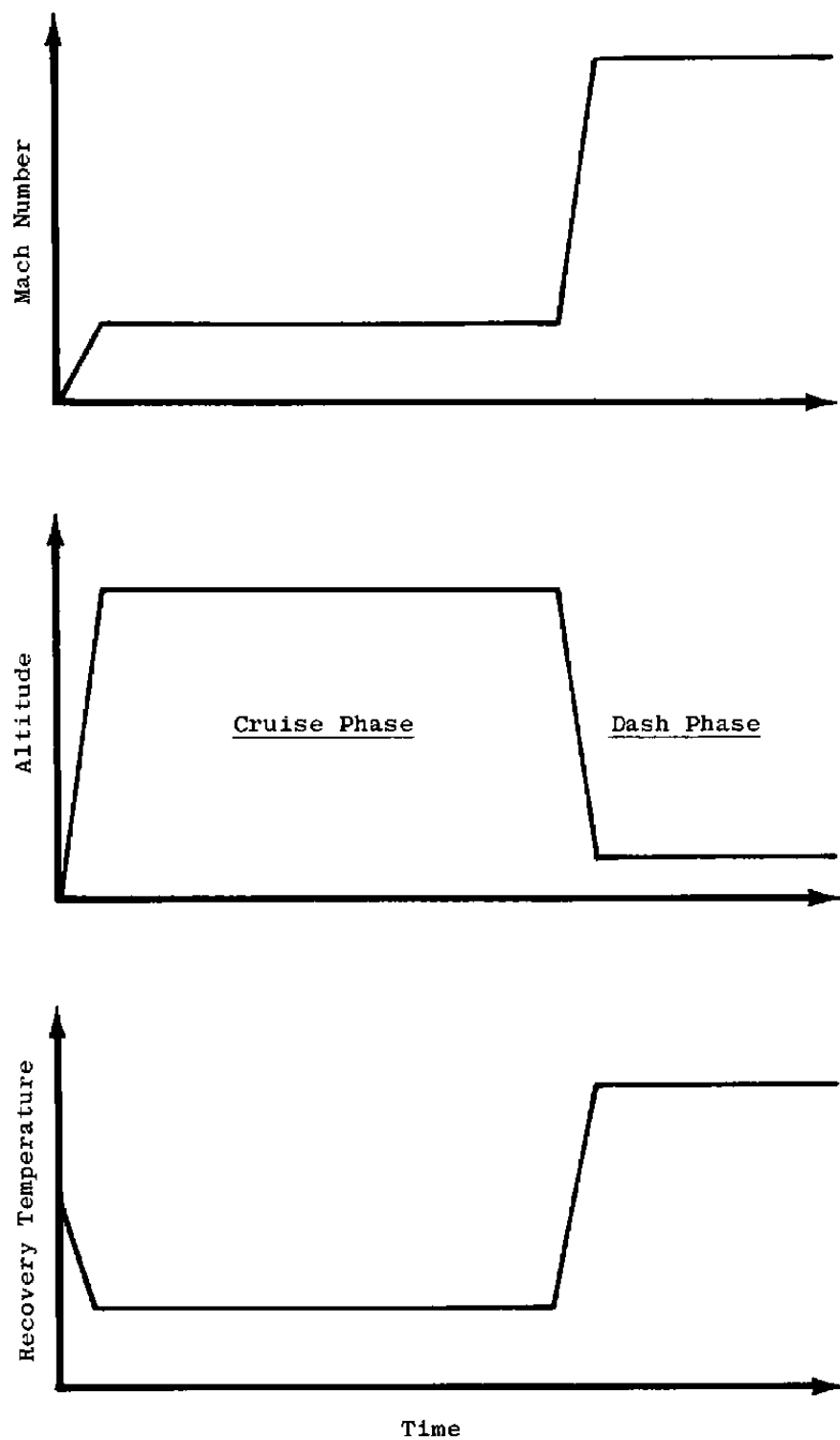
Figure 5. Mathematical model hypothetical mission.
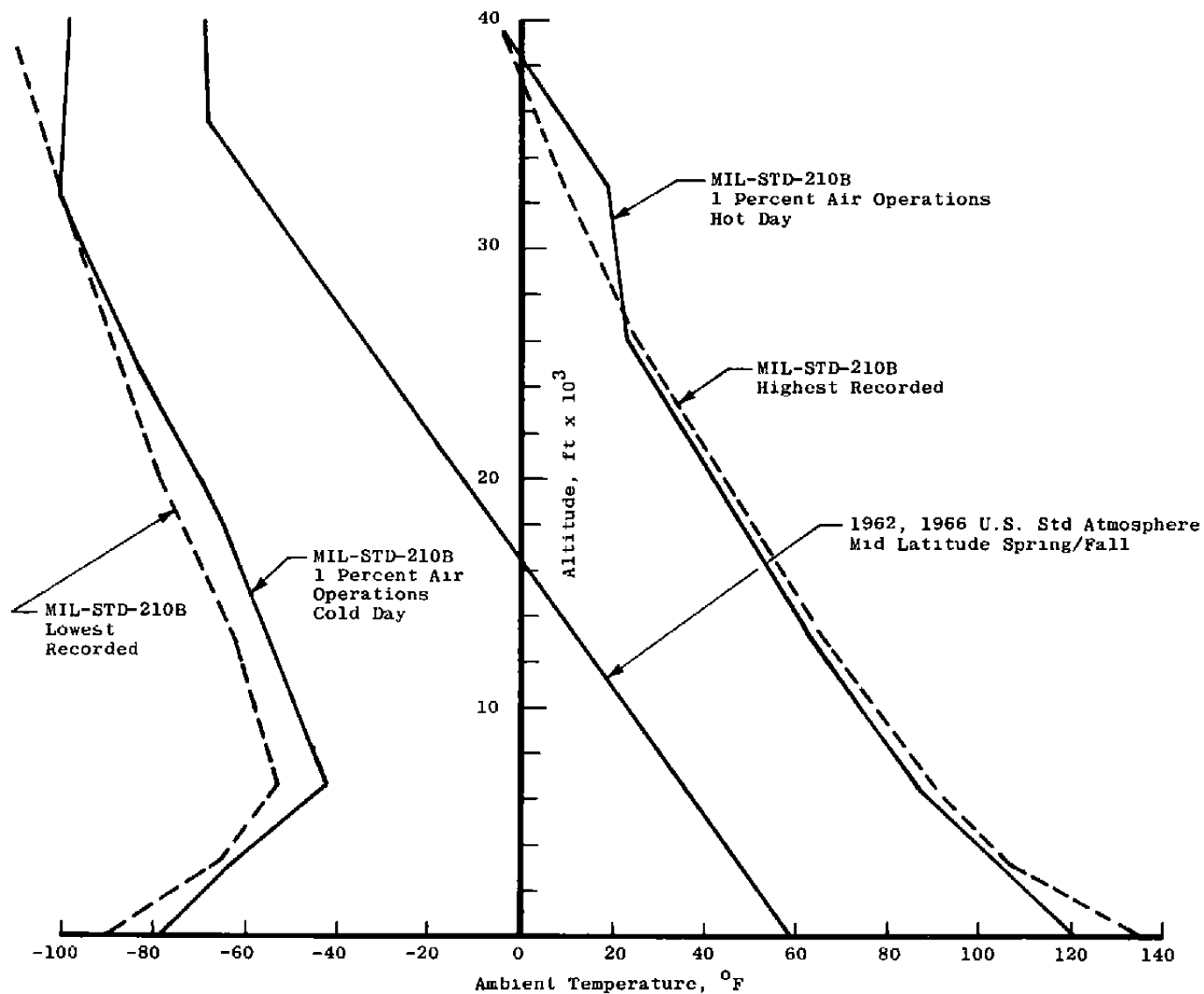
Figure 6. Ambient temperature variation with altitude.
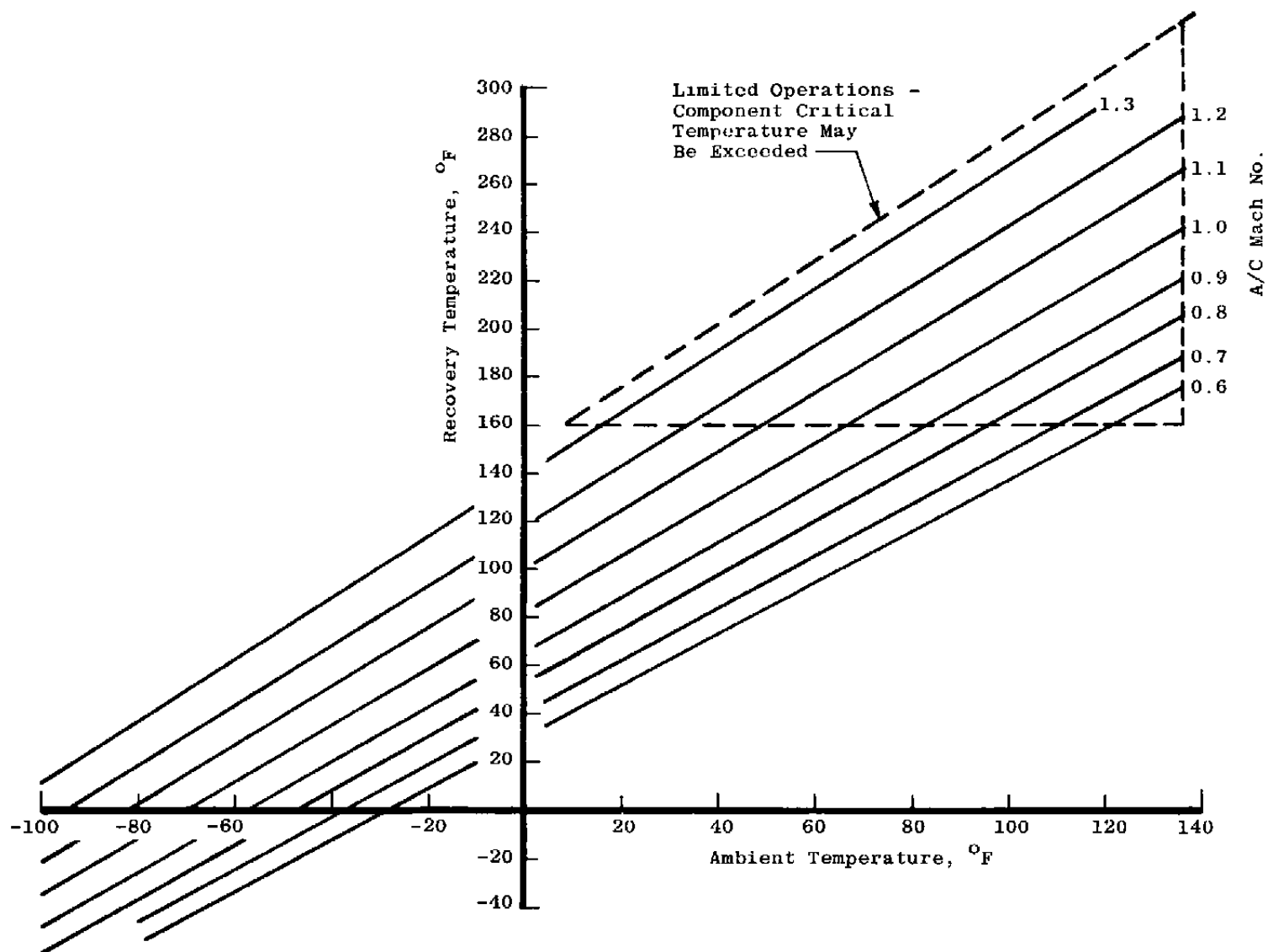
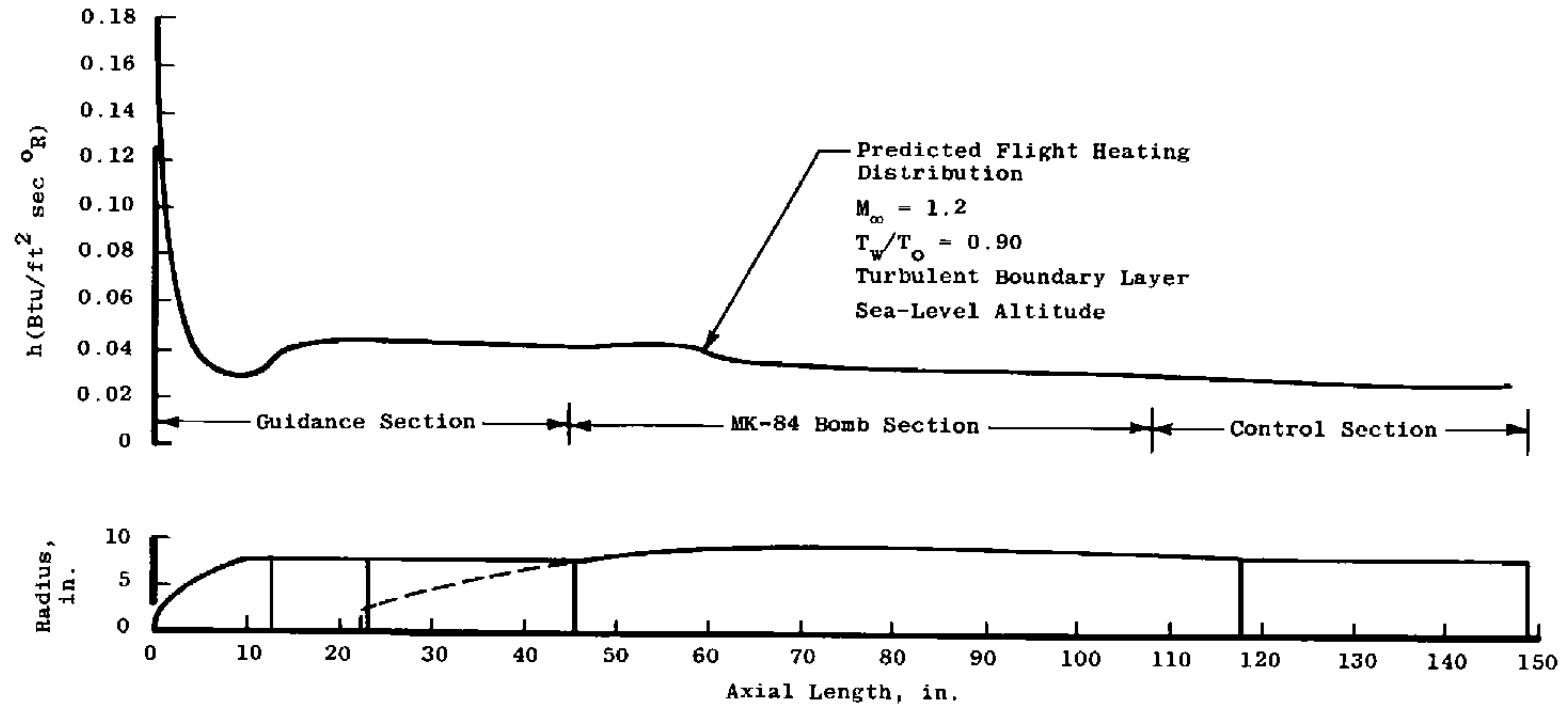Figure 7. Maximum possible store equilibrium temperatures.
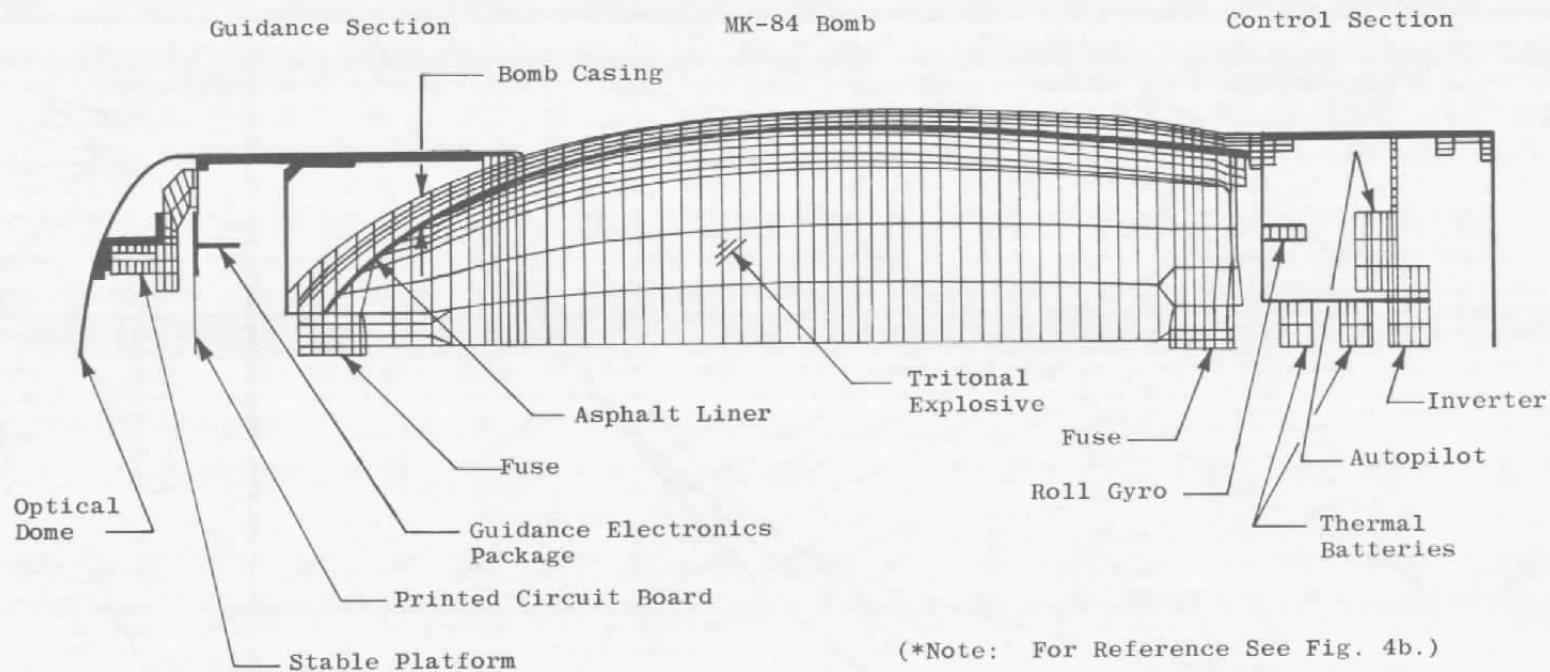
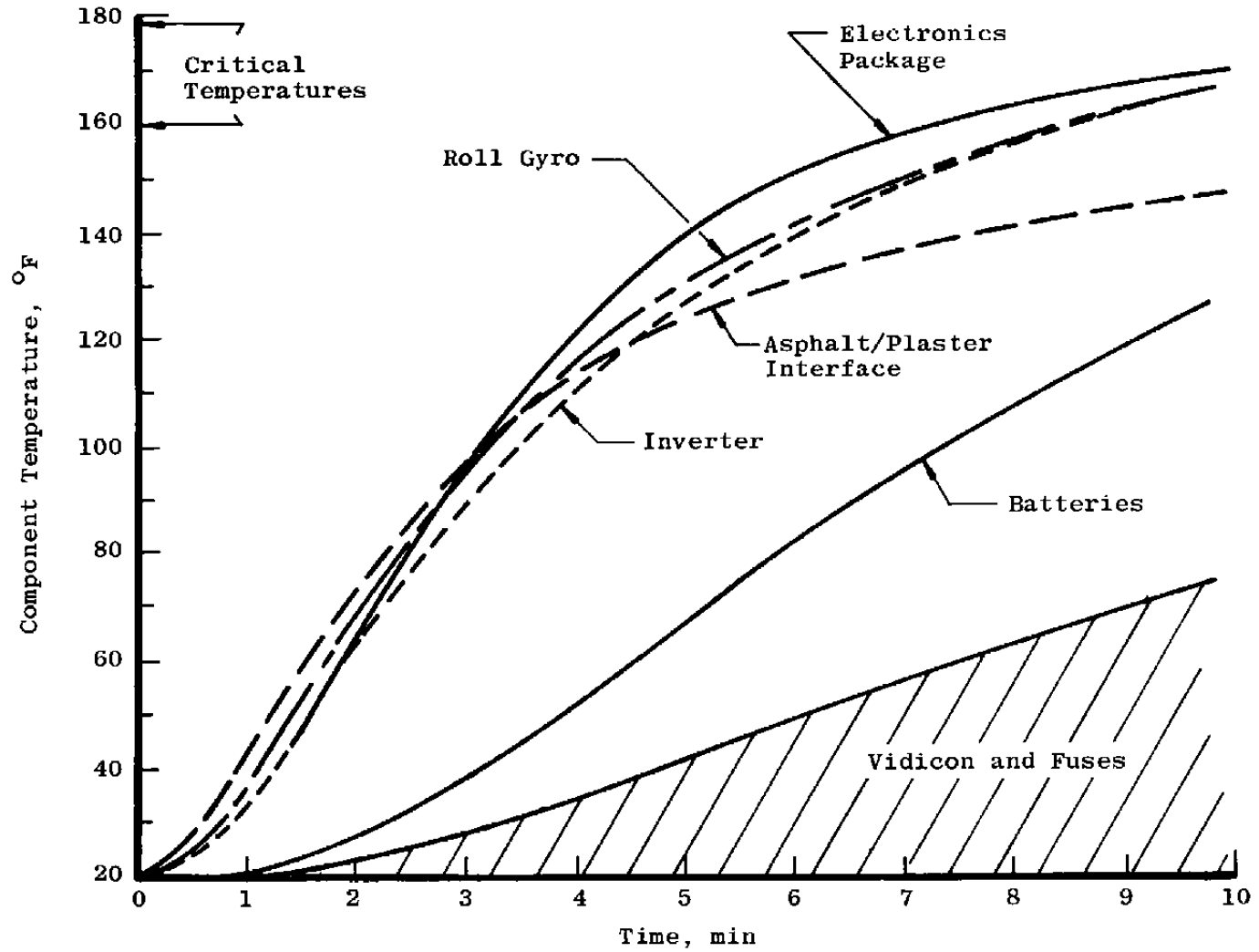Figure 8. GBU-8 and associated heating distribution.

Guidance Section                    MK-84 Bomb                    Control Section

— Bomb Casing

— Tritonal Explosive

— Asphalt Liner

Fuse —

— Fuse
Roll Gyro —

Optical Dome —

— Guidance Electronics Package

— Printed Circuit Board

— Stable Platform

— Inverter

— Autopilot

— Thermal Batteries

(*Note:  For Reference See Fig. 4b.)

Figure 9.  GBU-8 finite element model.

31

Figure 10. Component analytic thermal response.

External
Shroud

DANGER
HIGH
VOLTAGE

Test Article/Lamp
Support Chamber

A E D C
6436-78

Figure 11. Radiant-heat test stand and external shroud.

Figure 12. Mated shroud and test stand.

Lamp Holder

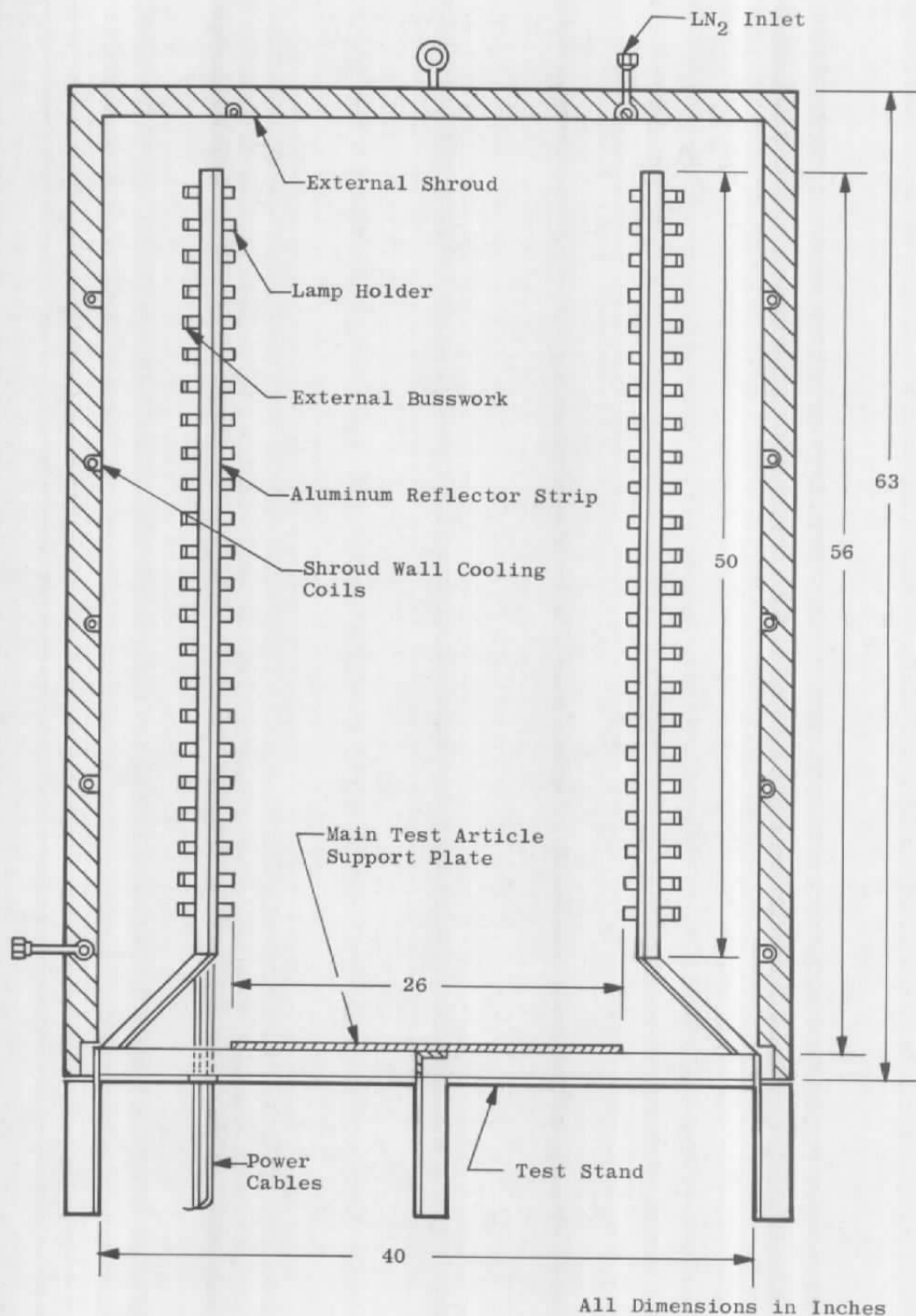Aluminum
Reflector
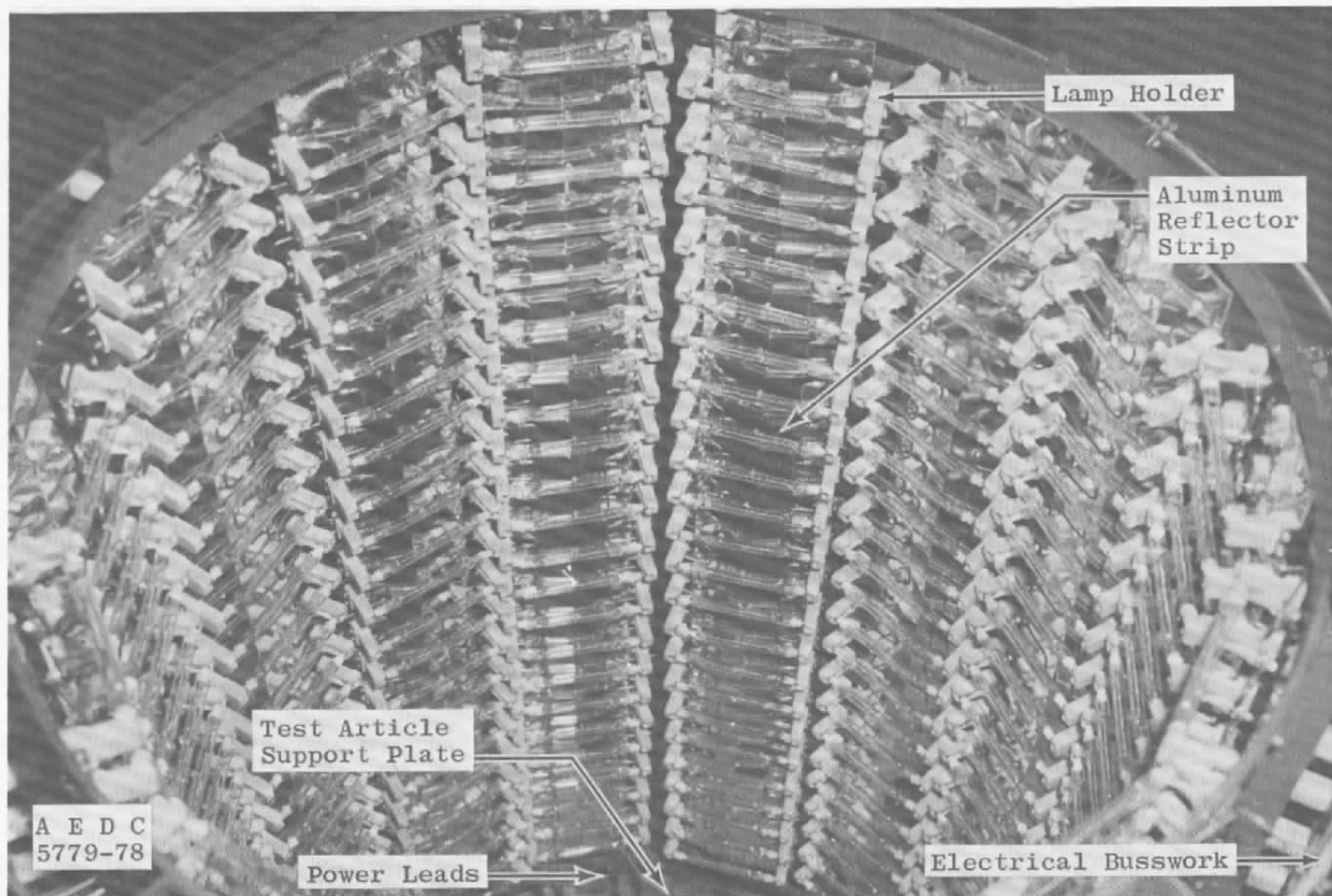Strip

Test Article
Support Plate

AEDC
5779-78

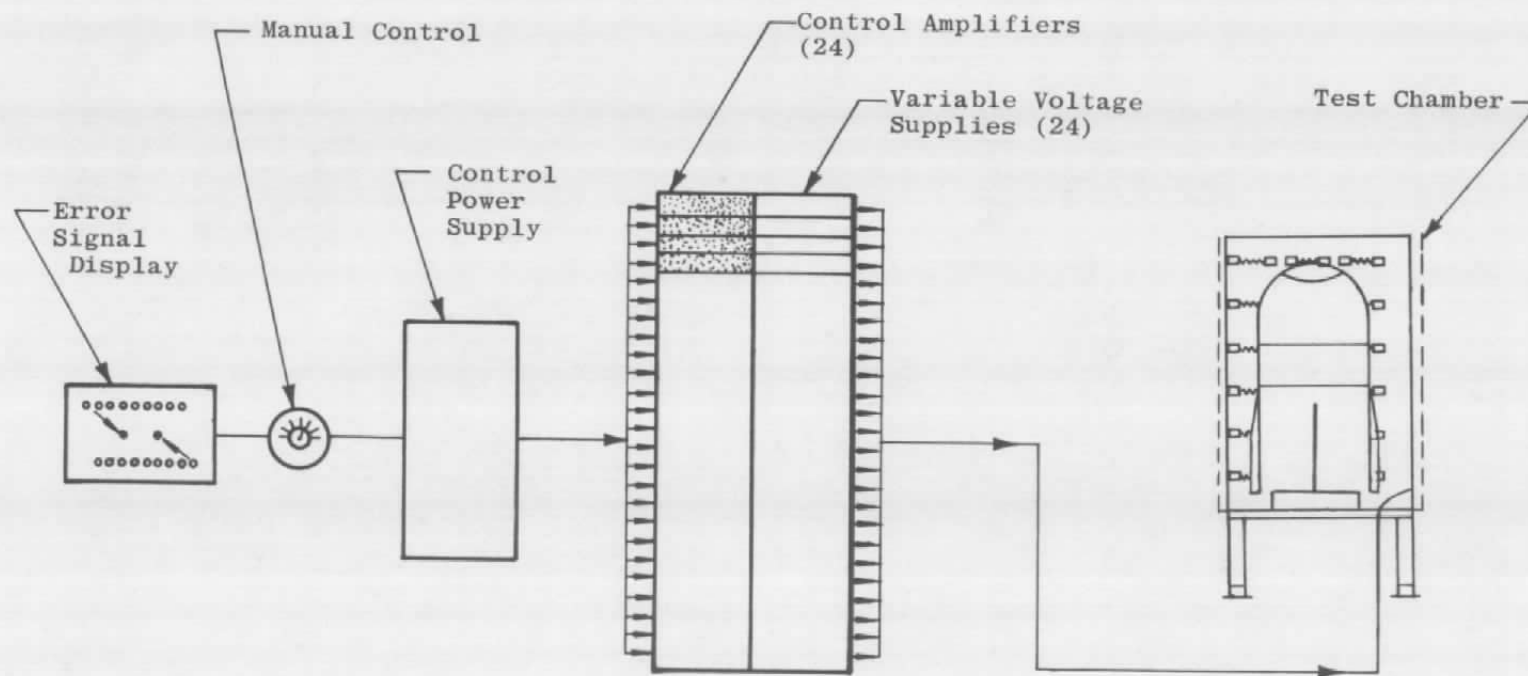Power Leads

Electrical Busswork

Figure 13. Lamp arrangement — test chamber interior.

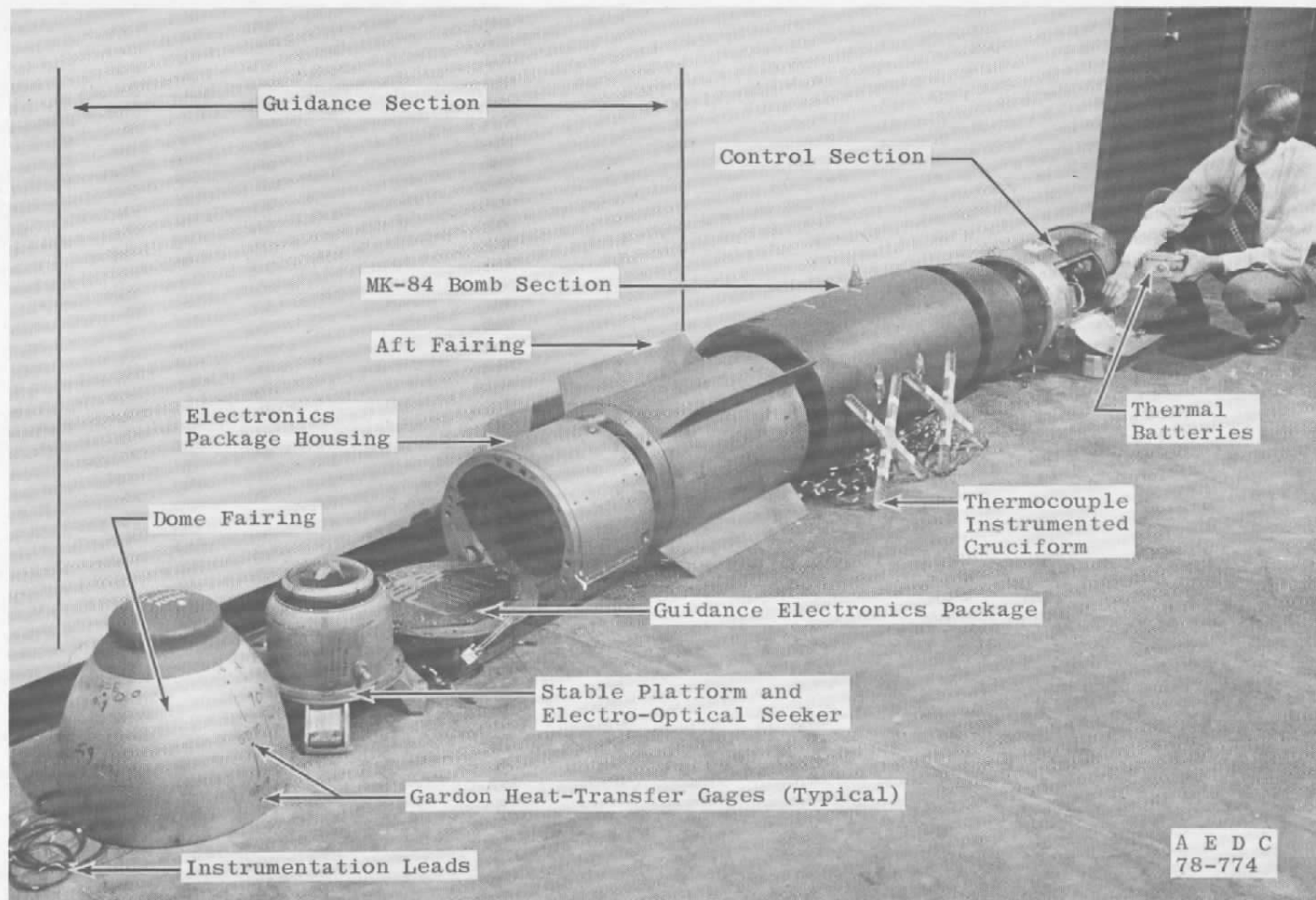Figure 14. Radiant-heat test unit electrical schematic.

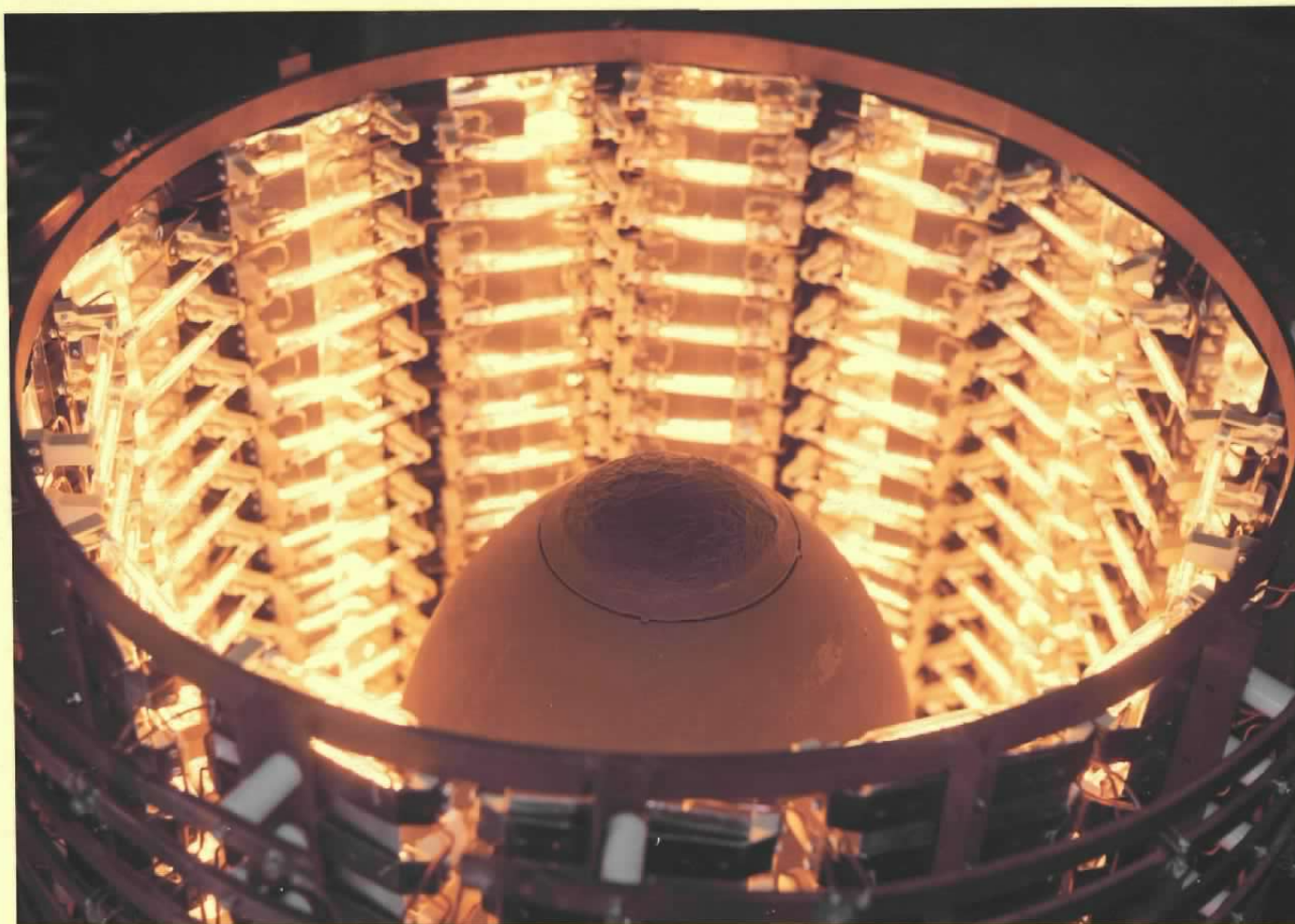Figure 15. Disassembled GBU-8 test hardware.

**Figure 16. Guidance section installation in the radiant-heat test chamber.**
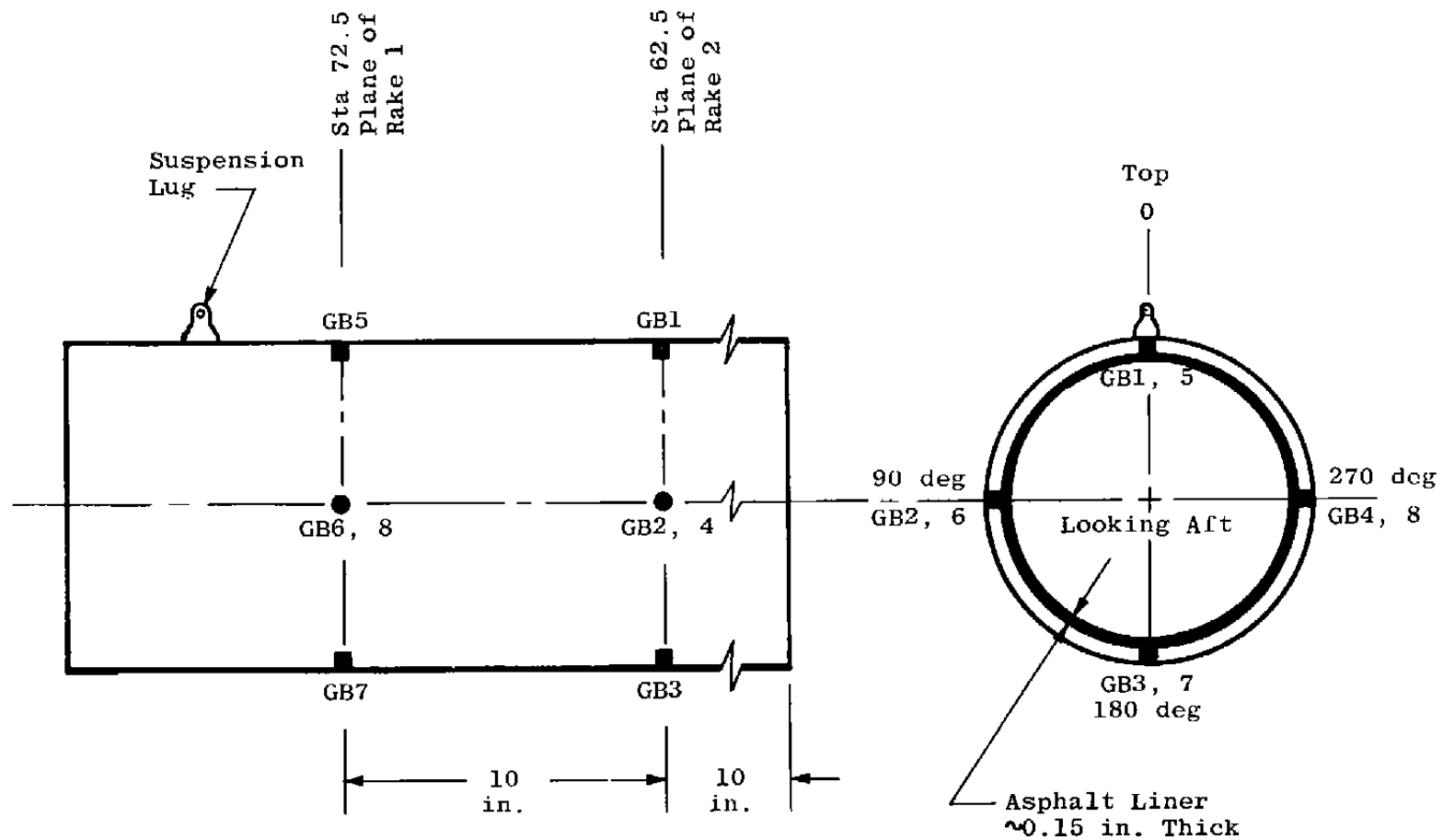
A E D C
6425–78

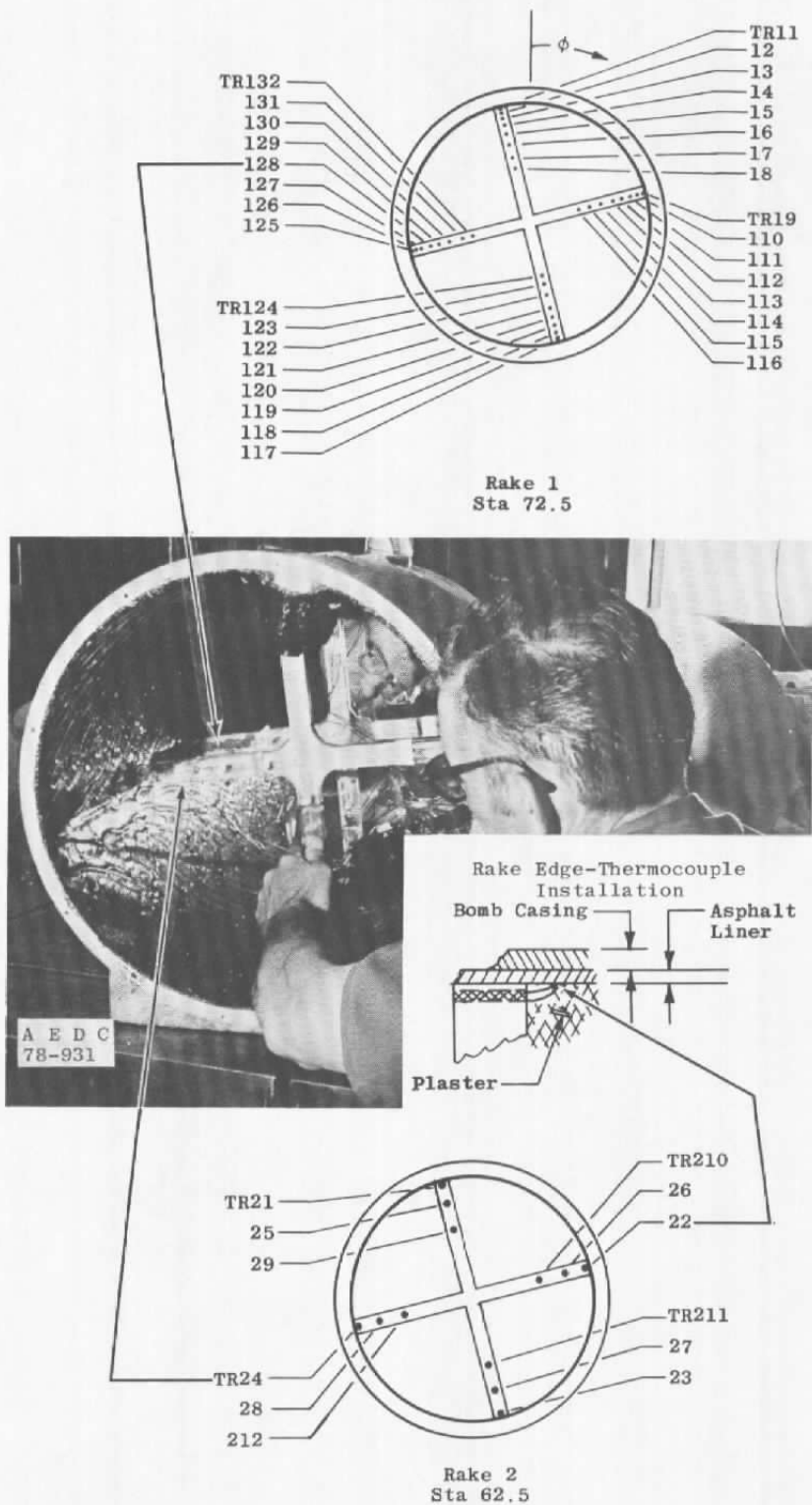Figure 17.  Bomb section heat-transfer gage locations.

Figure 18. Bomb section rake installation and thermocouple identification.

GD3, 7, 11,
15, 19, 23

180 deg

GD4, 8, 12,        GD2, 6, 10,
16, 20, 24         14, 18, 22

270 deg            90 deg

GD1

GD5

GD9

GD13

GD17

GD21

GD25

Vidicon Housing

Electronics Bay

Adaptor
Fairing

1.40

5.40

9.40

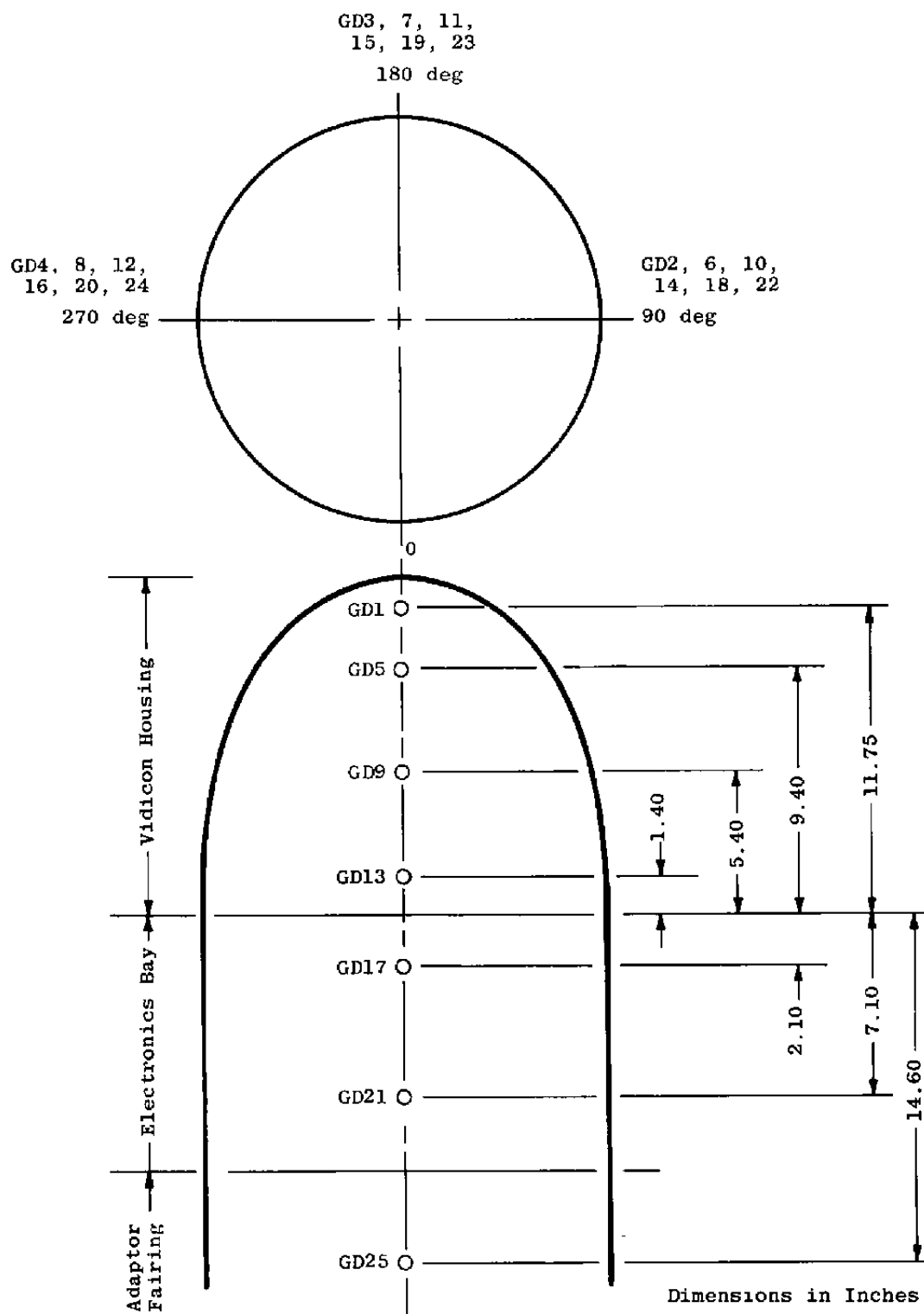11.75

2.10

7.10

14.60

Dimensions in Inches
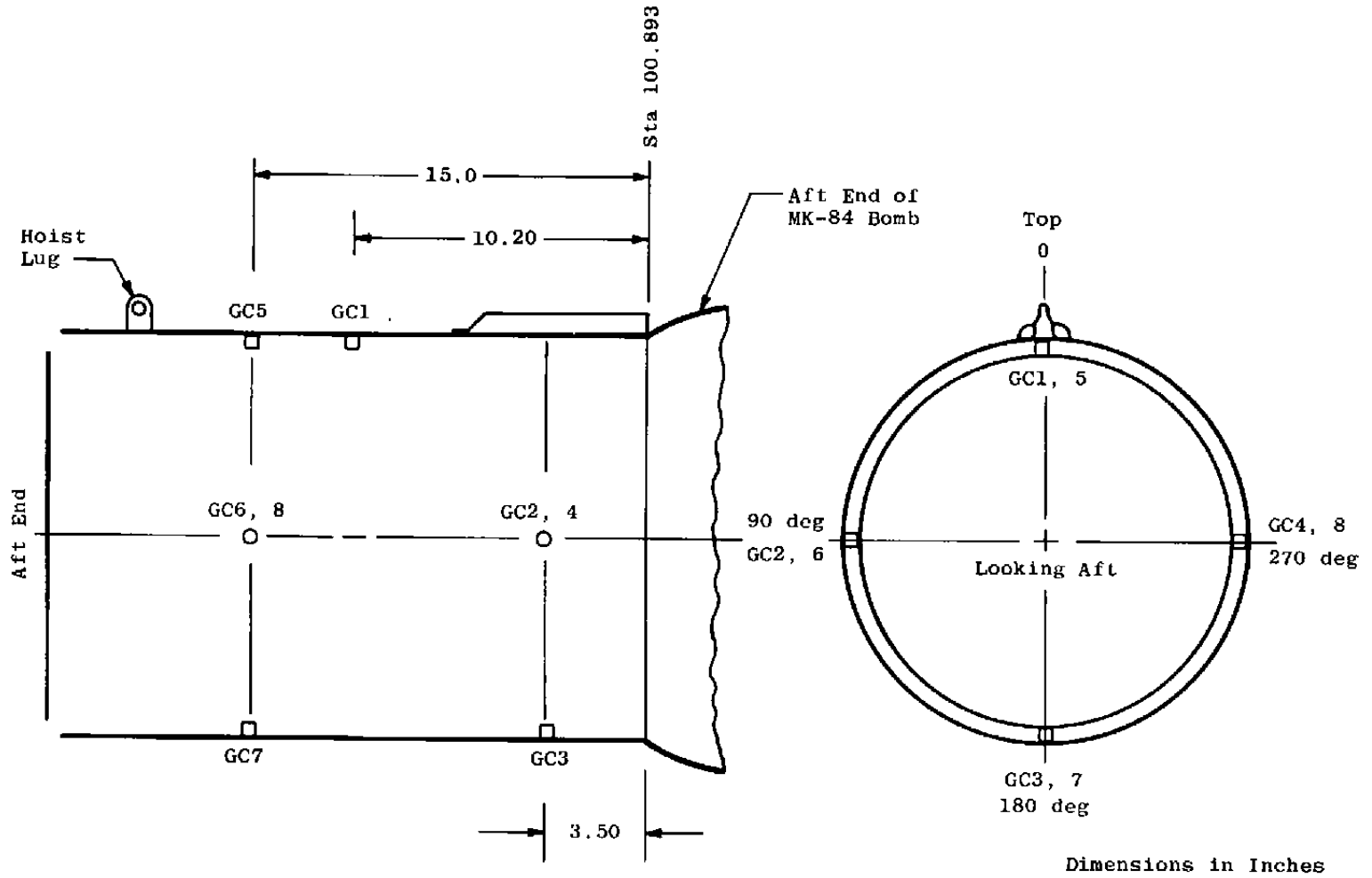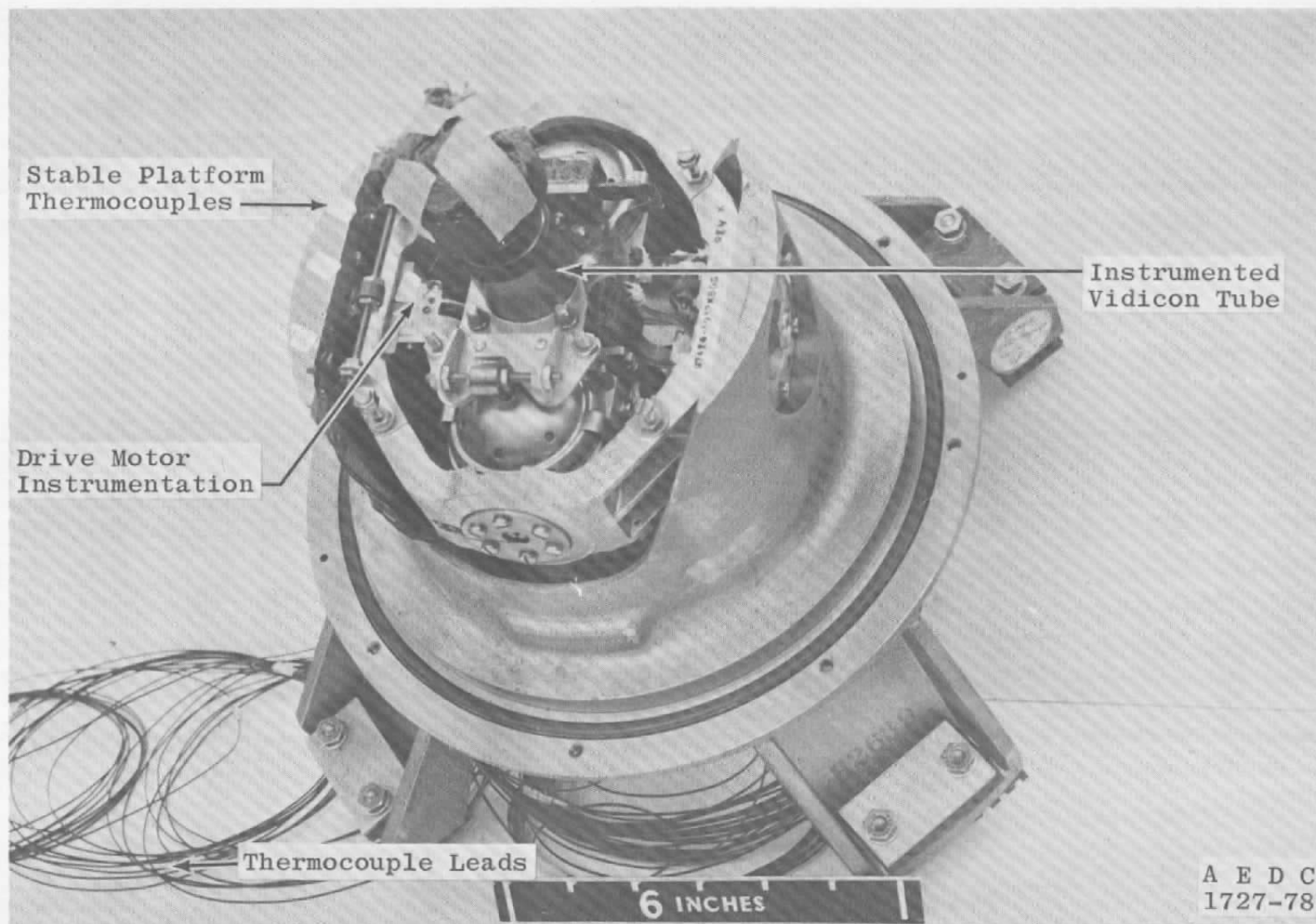
Figure 19. Guidance section heat-transfer gage locations.

Figure 20. Control section heat-transfer gage locations.

Stable Platform
Thermocouples →

Instrumented
Vidicon Tube

Drive Motor
Instrumentation

Thermocouple Leads

6 INCHES

A E D C
1727-78

a. Stable platform
Figure 21. Guidance section thermocouple instrumentation.

Instrumented Printed
Circuit Card

Instrumented Case

Instrumented
Component

Thermocouple
Leads

6 INCHES

AEDC
1731-78
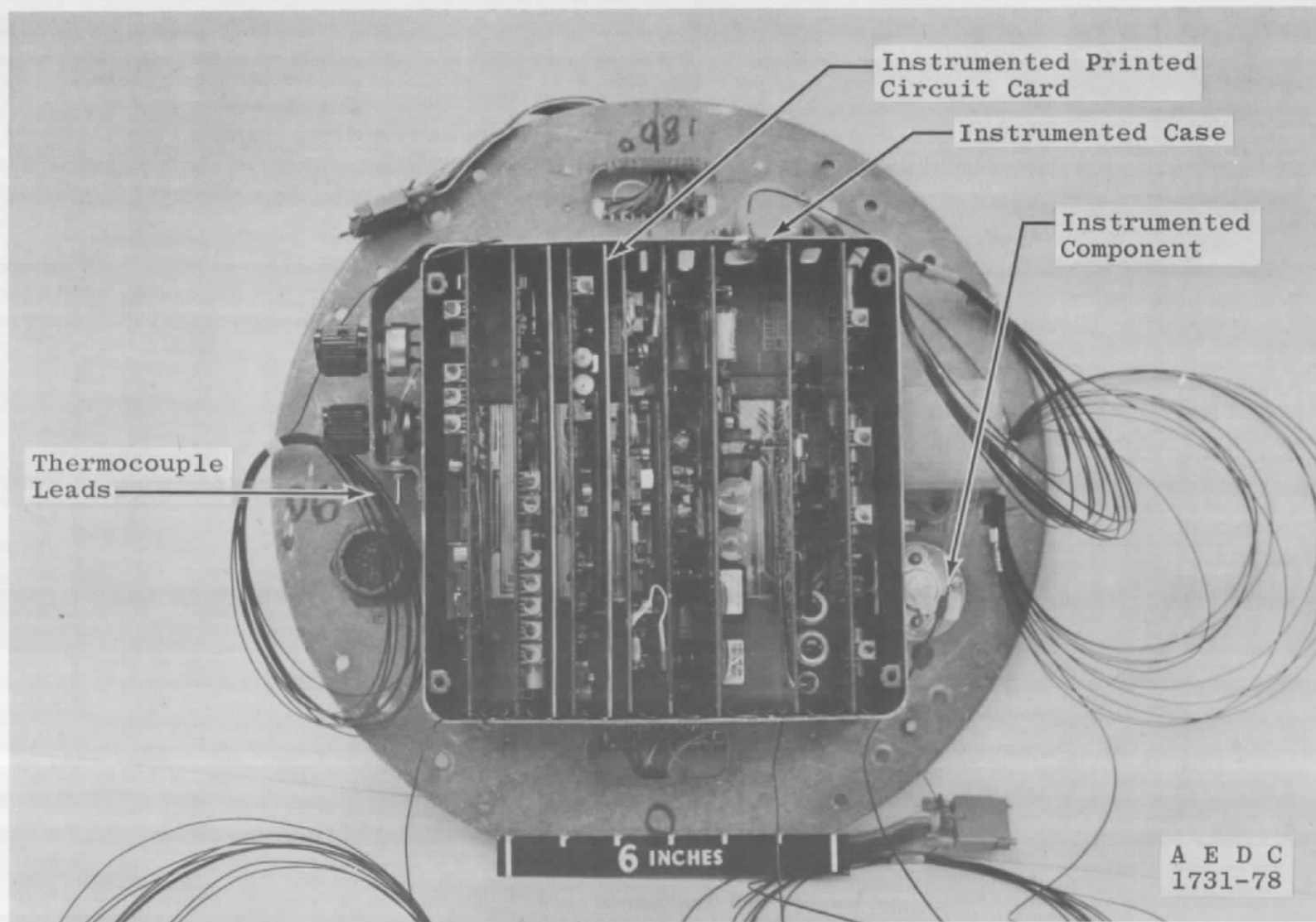
b. Guidance electronics
Figure 21. Concluded.

Battery Tray

Power Inverter

Thermal Battery

Autopilot

Thermocouple Leads

AEDC
2856-78
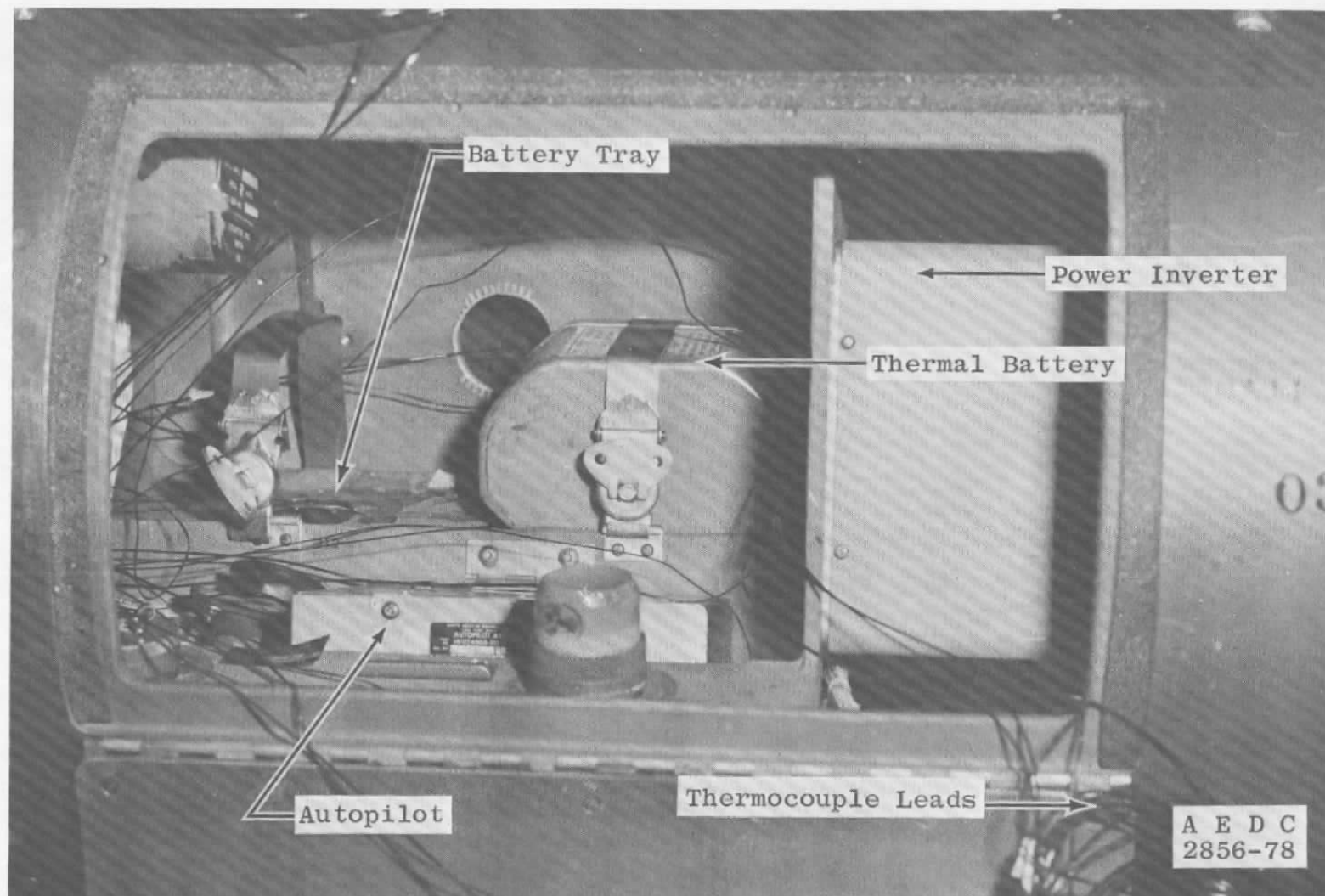
a. Battery autopilot and power inverter
Figure 22. Control section thermocouple instrumentation.

Gardon Gage Installation

Roll Gyro Thermocouple

External Case Thermocouples (Attachment with Conductive Epoxy)

A E D C
2854-78
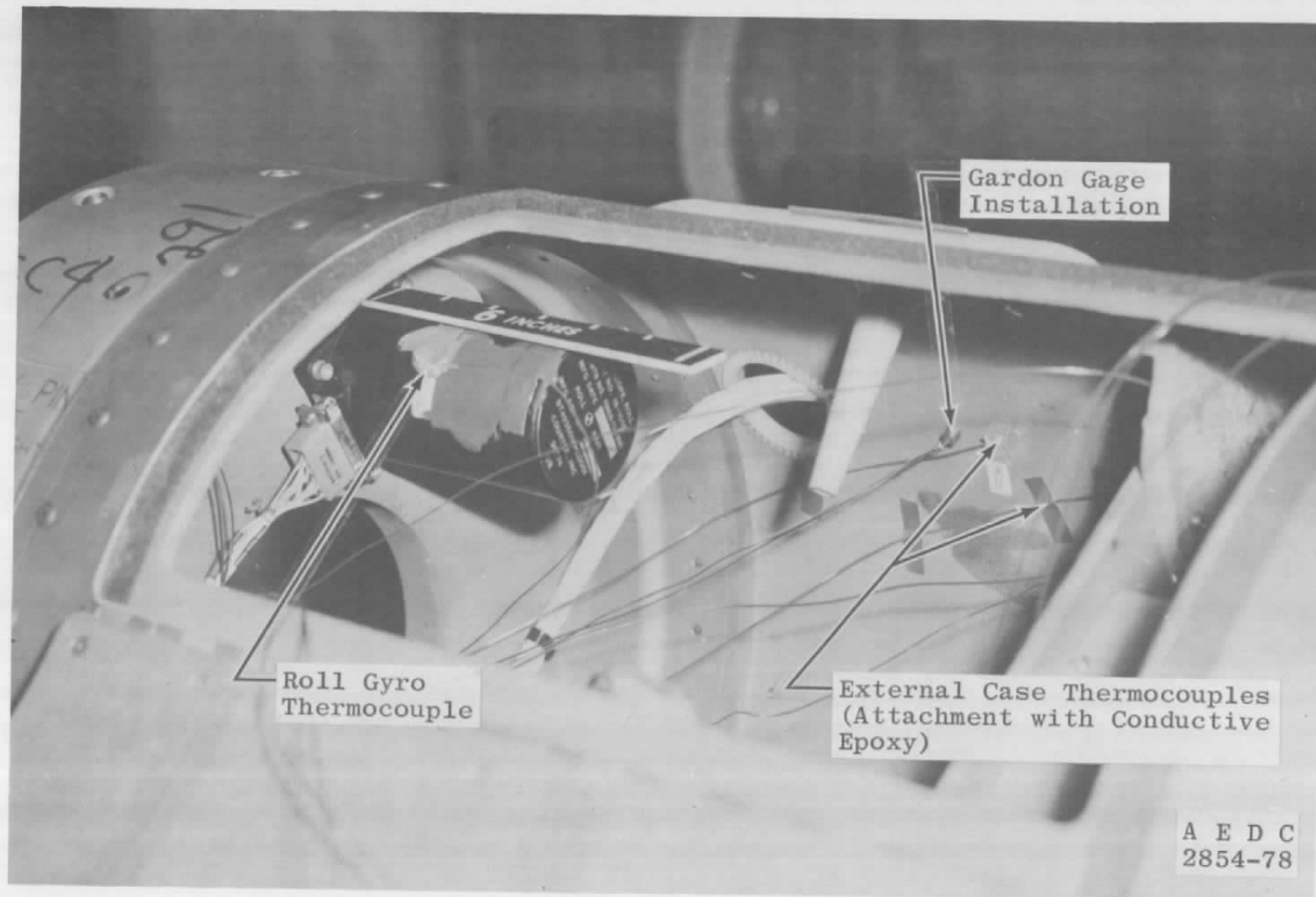
b.  Roll gyro and external case
Figure 22.  Concluded.

Predicted
Flight
Heating
Inputs

$h, T_r$                                              $h_{in}$

$\dot{q}_{meas}, T_{wall}$  $\longrightarrow$  $\dfrac{\dot{q}_{meas}}{(T_r - T_w)}$  $\longrightarrow$  $h_{out}$

$\dot{q}_{meas}, T_{wall}$

80 70 60 50 40 30 20 10 5  +
o  o  o  o  o  o  o  o  o
Error          ●  ●          Display
o  o  o  o  o  o  o  o  o
−  5 10 20 30 40 50 60 70 80
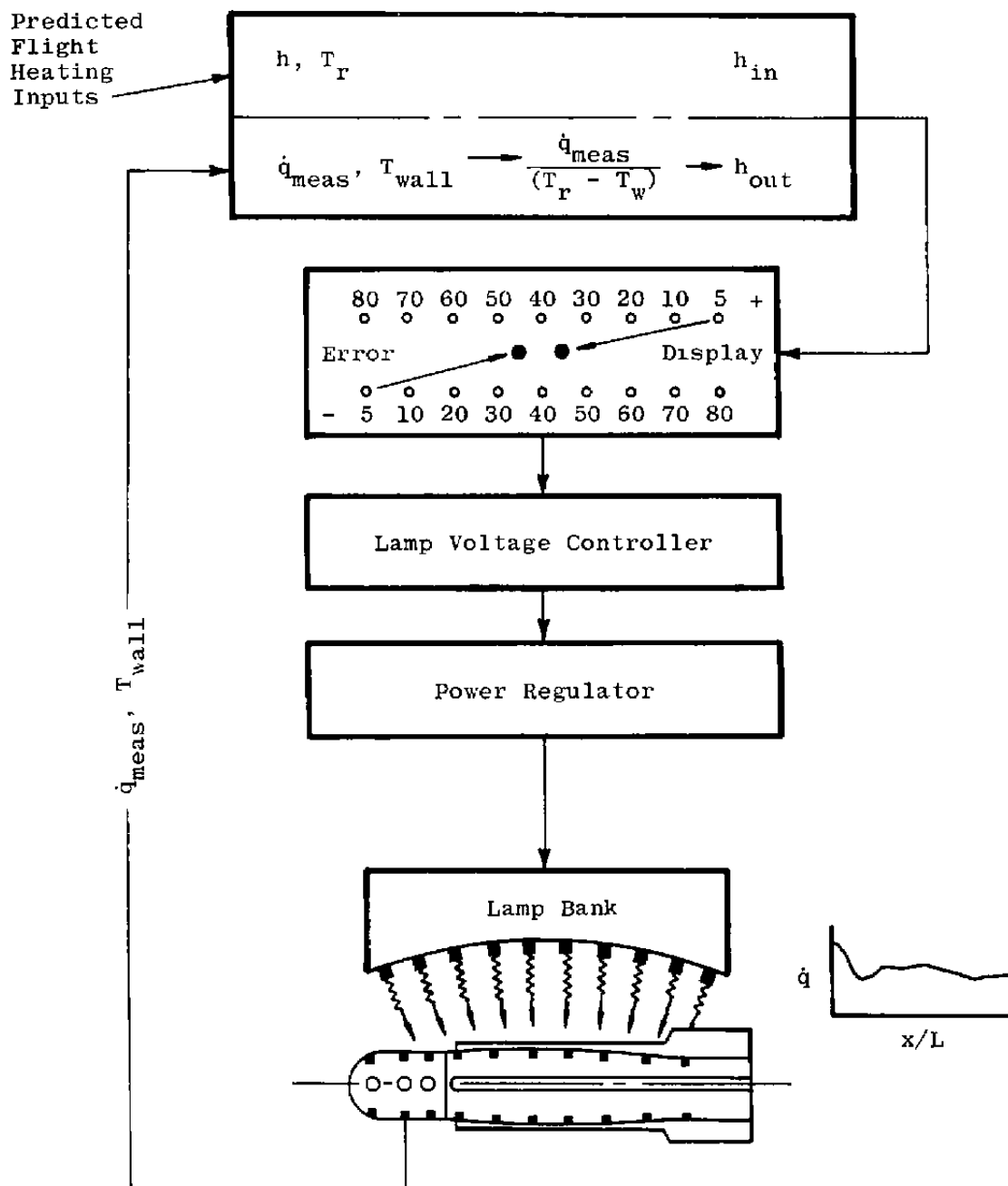
Lamp Voltage Controller

Power Regulator

Lamp Bank

$\dot{q}$

x/L

Figure 23.  Radiant-heat test philosophy.

49
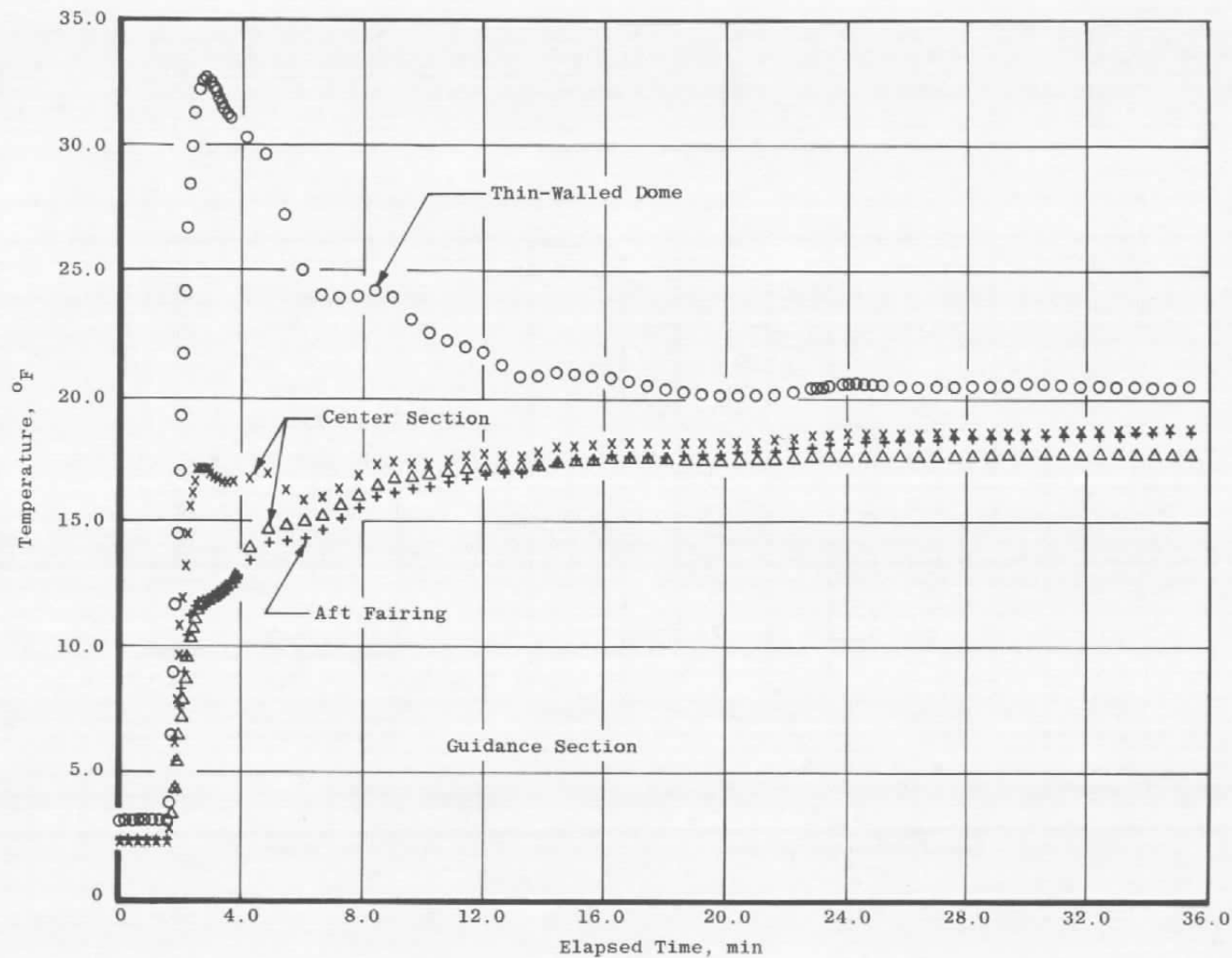
Figure 24. Wall thickness effect on heating rate control philosophy.

a. Heating rate — $\dot{q}$    b. Wall temperature — $T_w$
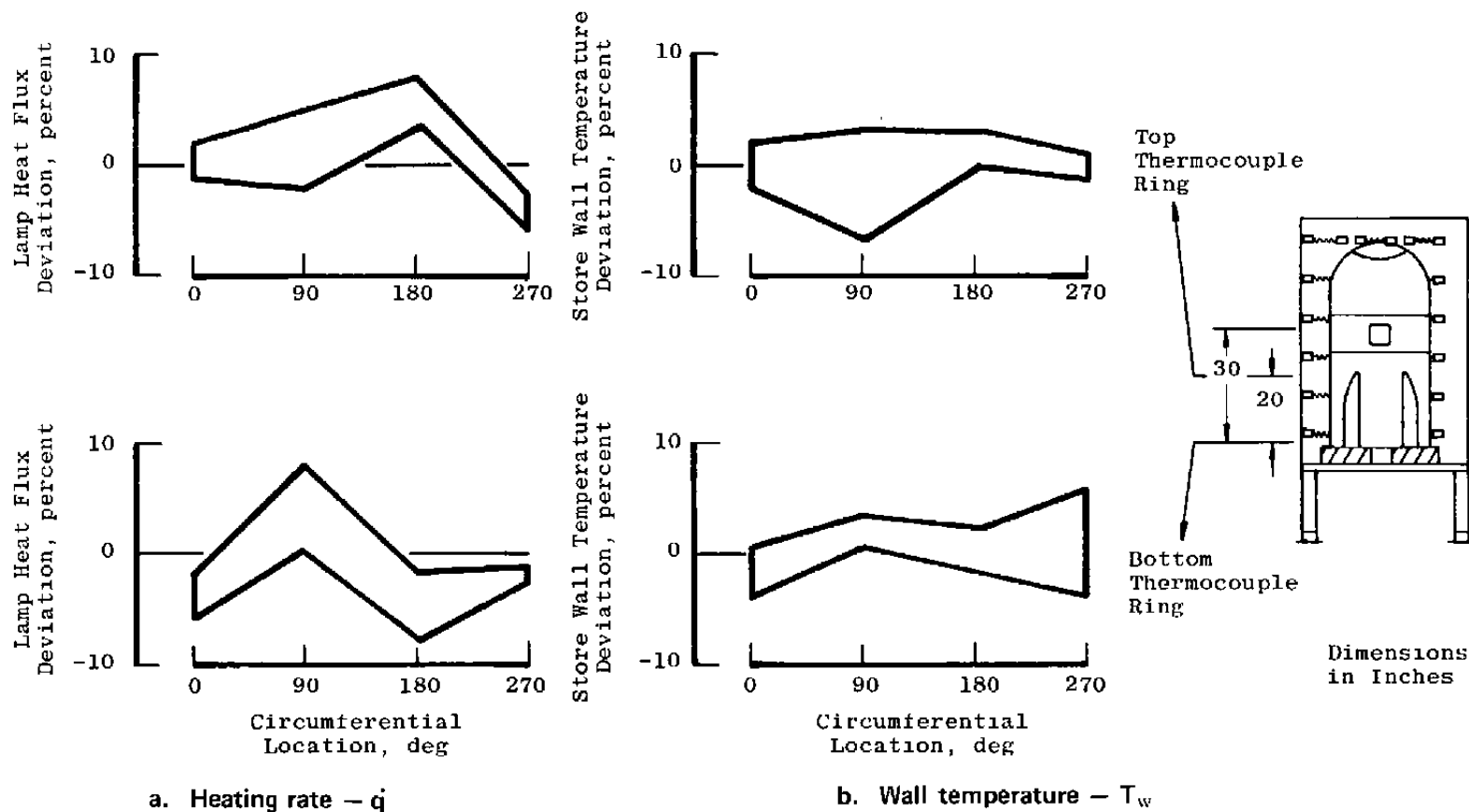
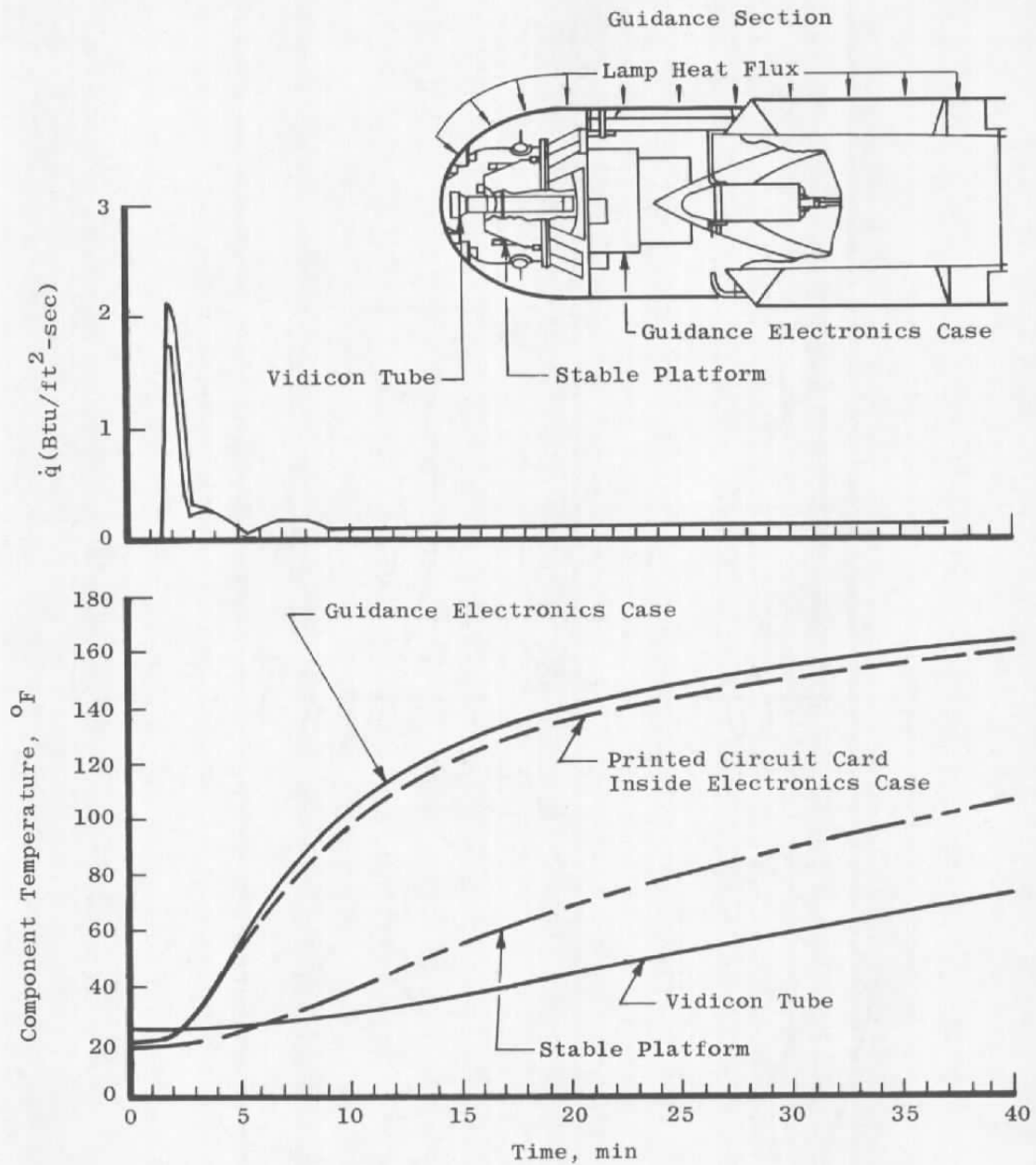Figure 25.  Test cell spatial heating uniformity.
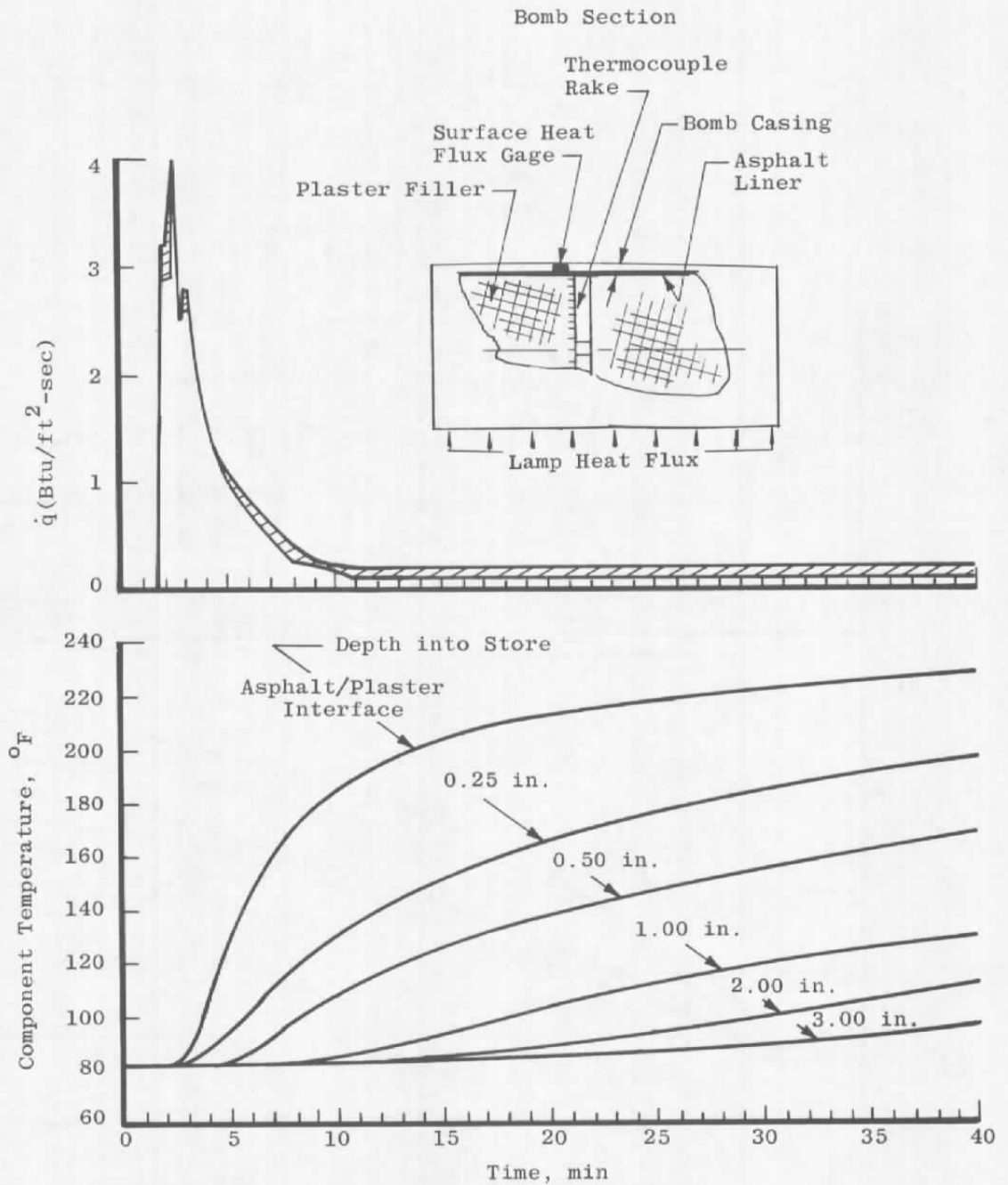
Figure 26. Ground test results — guidance section.

Figure 27. Ground test results — MK-84 bomb section.

53
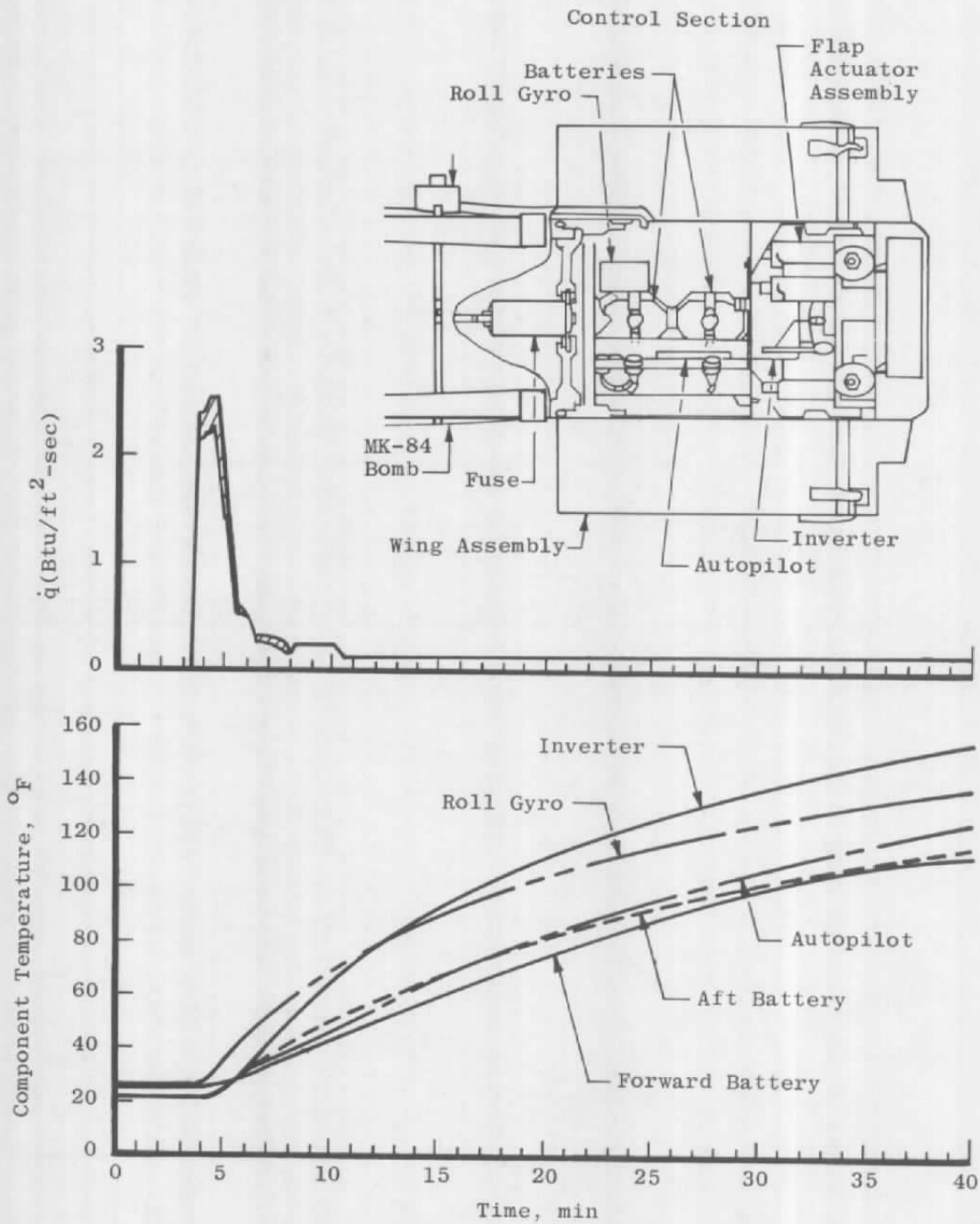
Figure 28. Ground test results — control section.

a. Guidance section



b. Bomb section

Figure 29. Ground test thermal response for the GBU-8 guidance, bomb, and control sections.

c. Control section

Figure 29. Concluded.

Figure 30.  Bomb section circumferential thermal response.

a. Guidance section
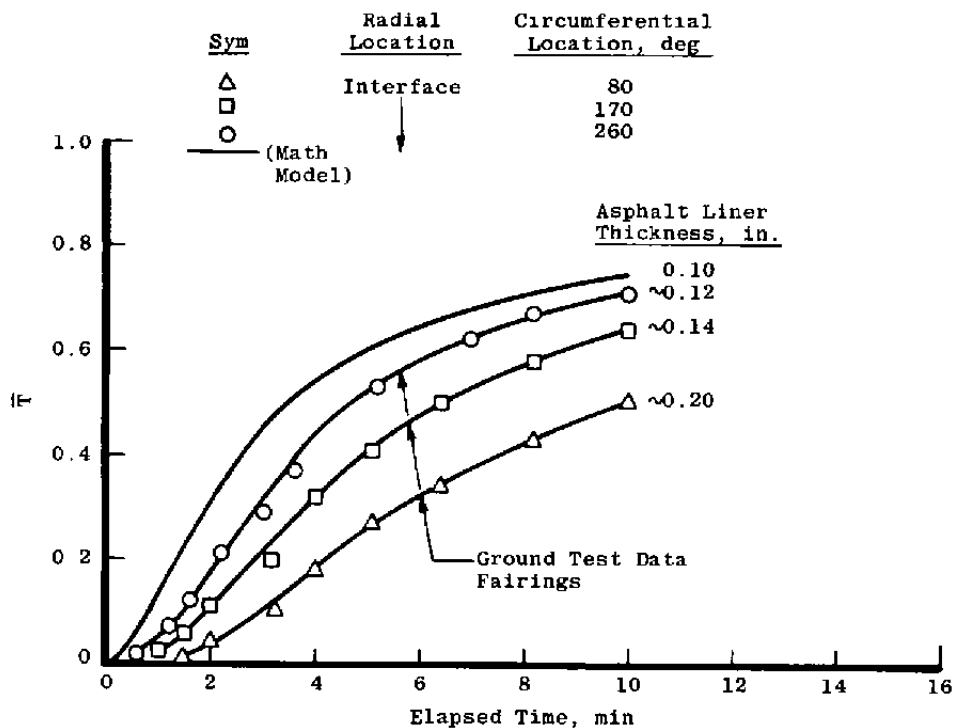


b. Bomb section

Figure 31. Comparison of analytic and ground test data.
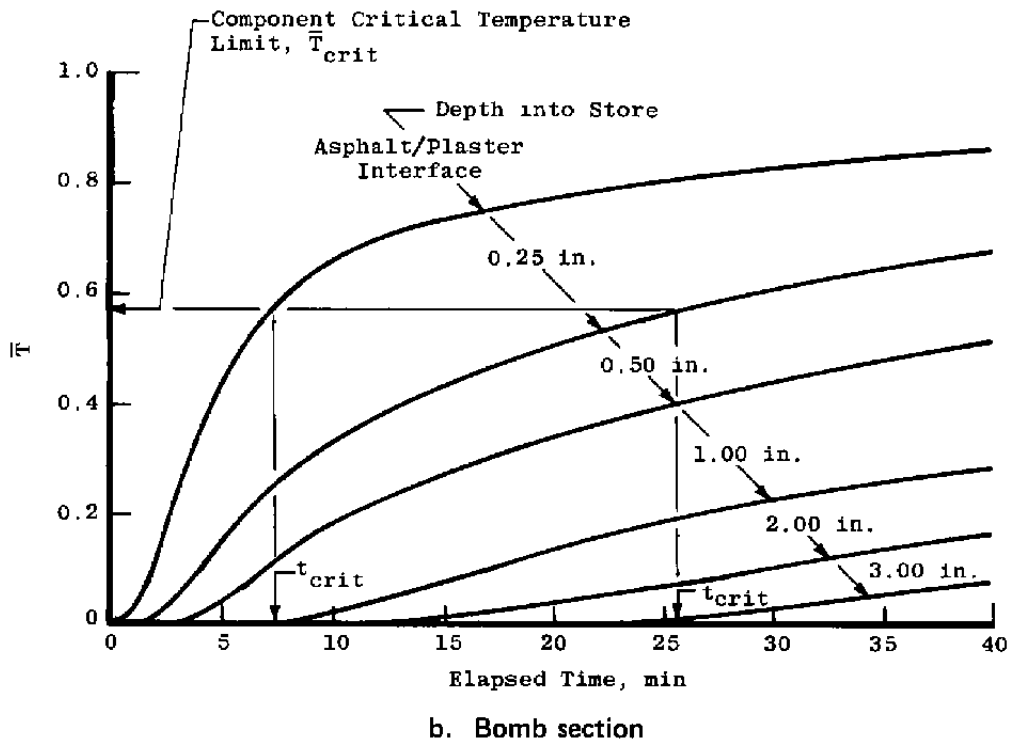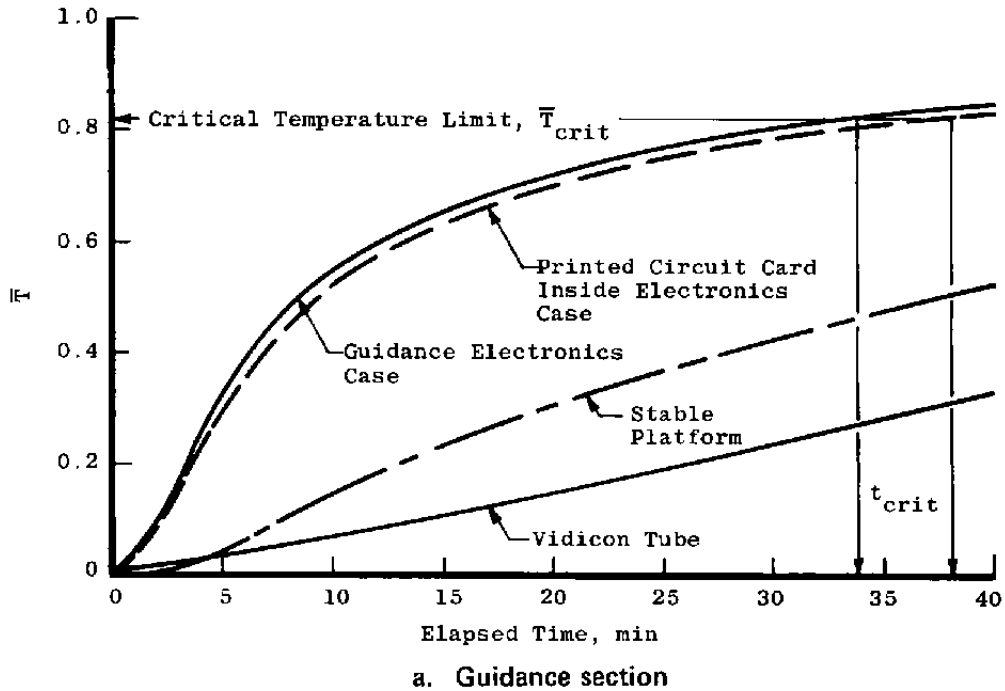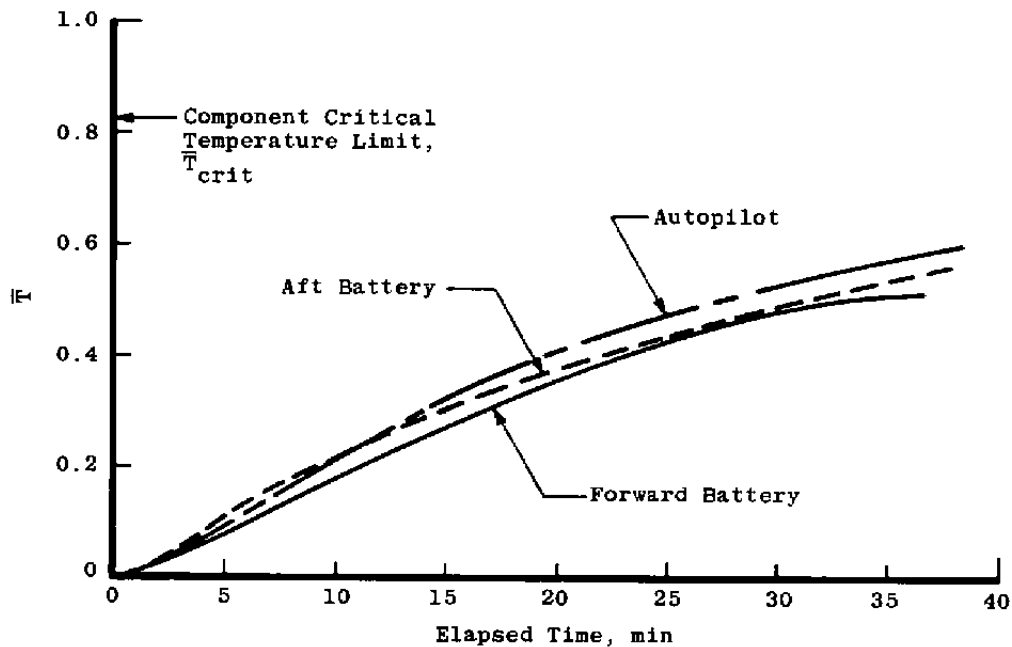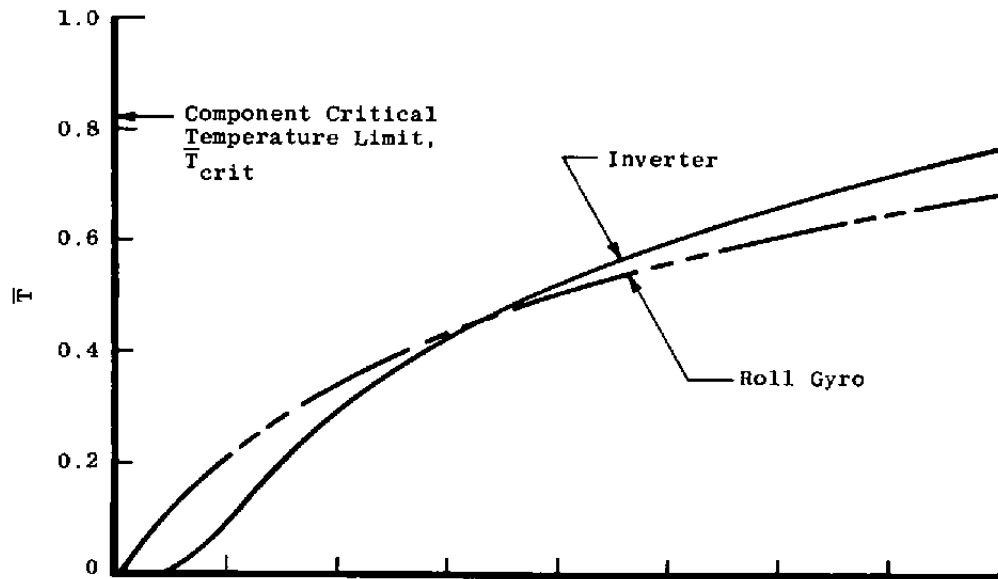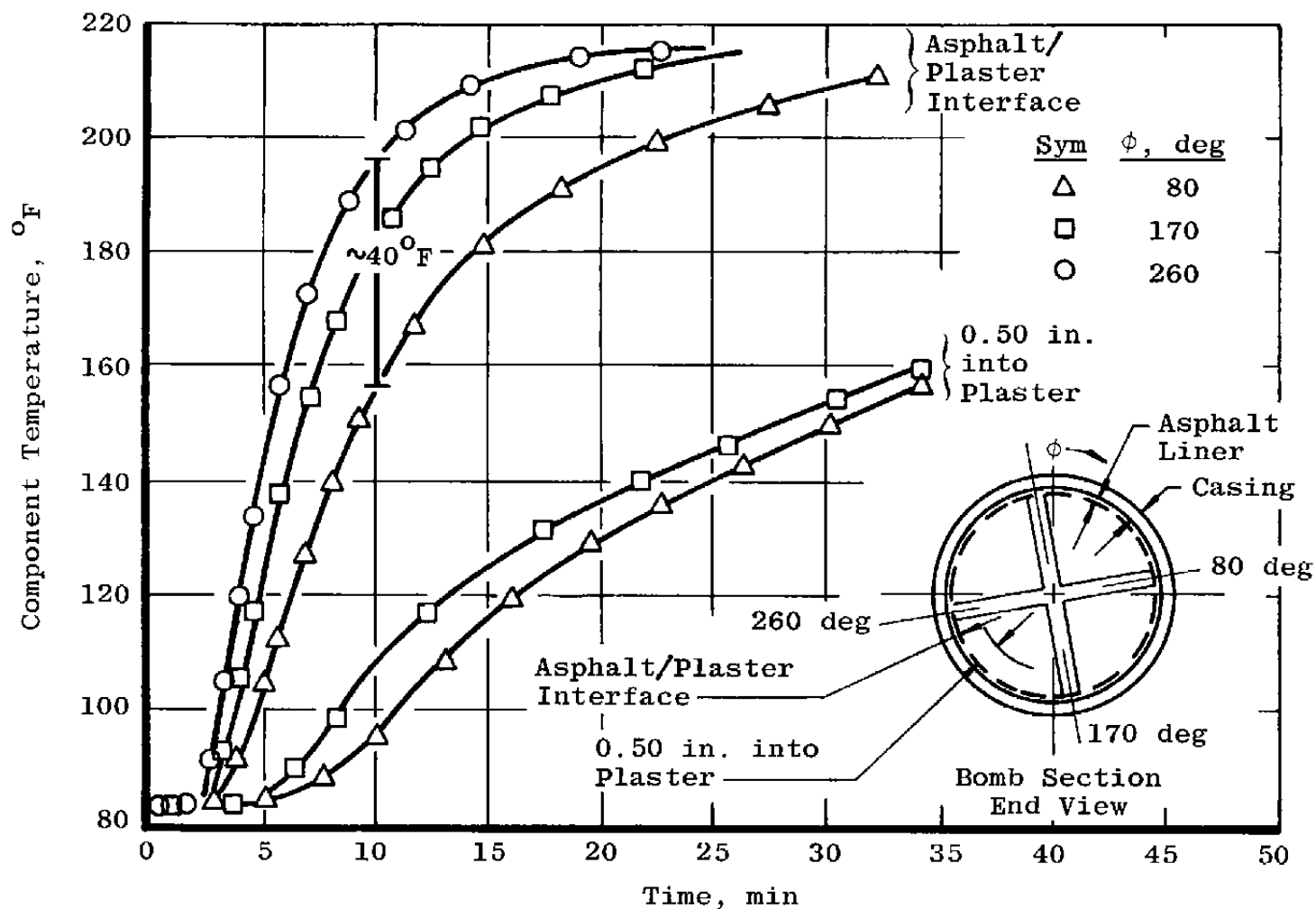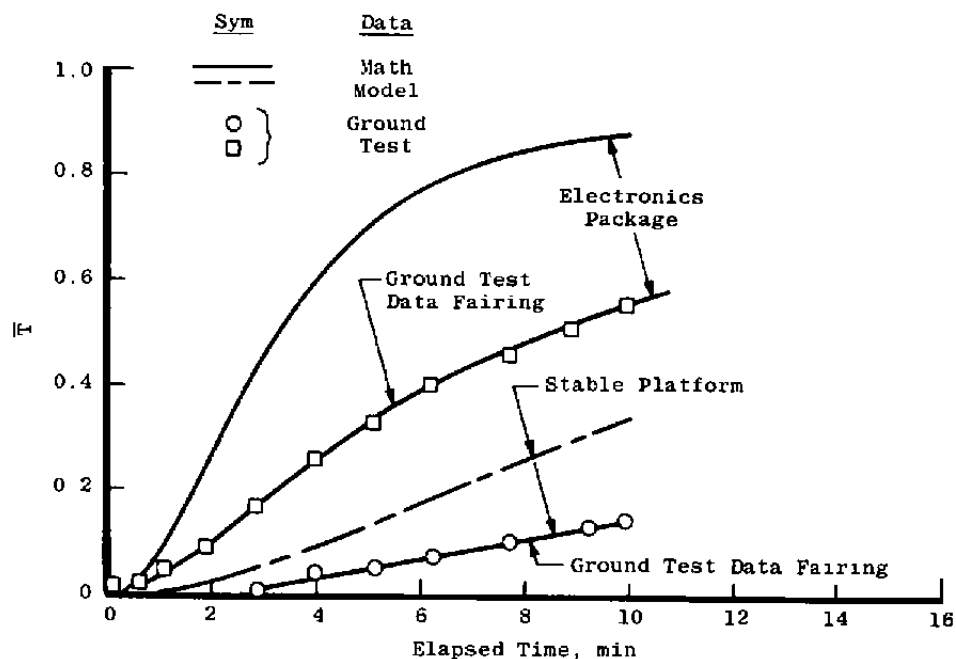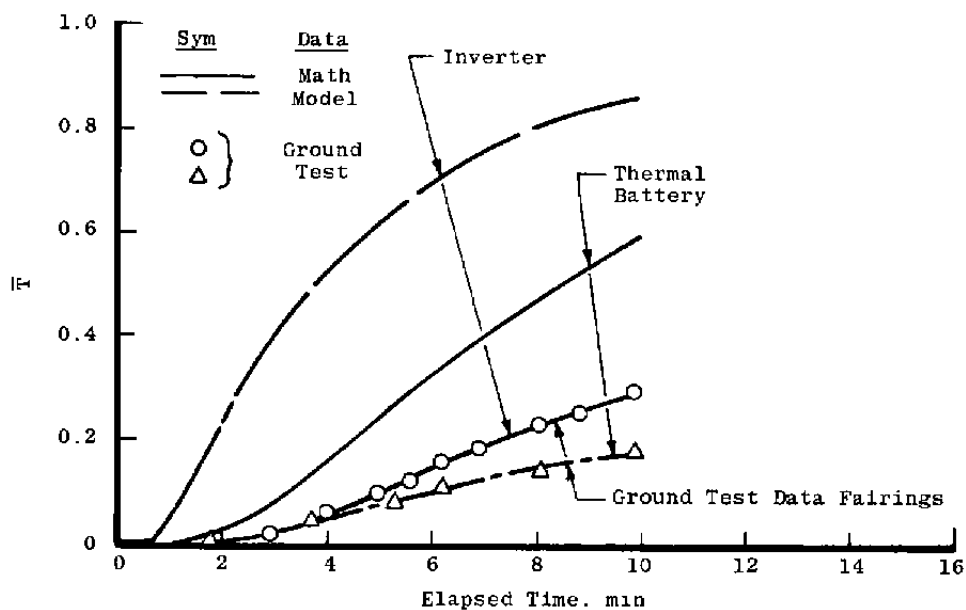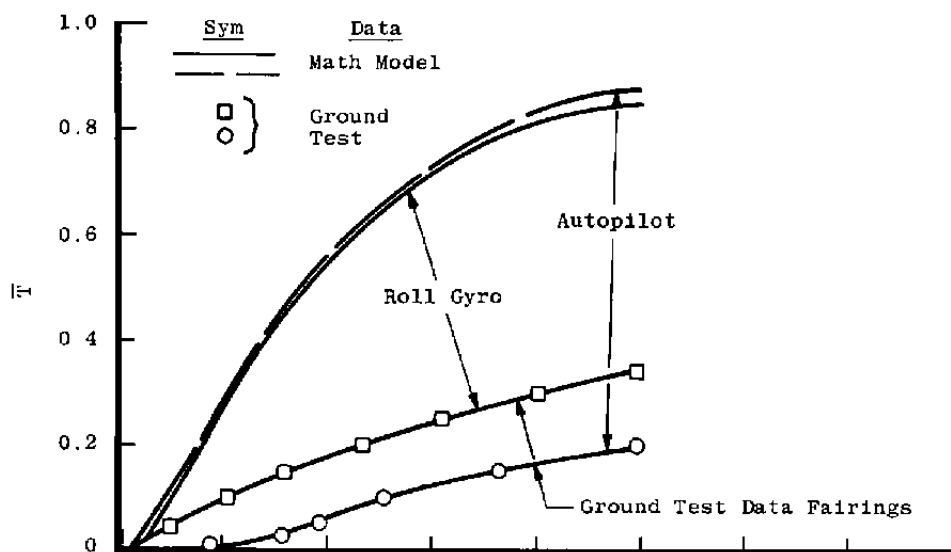
c. Control section
Figure 31. Concluded.

Table 1. GBU-8 Material and Thermal Properties Summary

| Section | Component | Material | $\rho$, lbm/in.$^3$ | $C_p$, Btu/lbm-°F | $k$, Btu/in.-min-°F |
|---|---|---|---|---|---|
| Guidance | Optical Dome | Optical Glass | 0.091 | 0.205 | 0.00089 |
| | Exterior Case and Bulkheads | 6061 – T6 Al. Sh | 0.098 | 0.230 | 0.1380 |
| | | 356 – T51 Al. Alloy | 0.098 | 0.230 | 0.1380 |
| | Stable Platform | A380 Al. Alloy | 0.098 | 0.230 | 0.1380 |
| | Guidance Electronics Case | 6061 – 0 Al. Sh | 0.098 | 0.230 | 0.1380 |
| MK-84 Bomb | Case | Steel | 0.285 | 0.120 | 0.0360 |
| | Asphalt Liner | Asphalt | 0.040 | 0.440 | 0.00018 |
| | Explosive | Dry Plaster | 0.055 | 0.230 | 0.00037 |
| Control | Exterior Case and Bulkheads | 356 – T51 Al. Alloy | 0.097 | 0.230 | 0.1380 |
| | Roll Gyro (Case) | 6061 – T6 Al. Alloy | 0.097 | 0.230 | 0.1380 |
| | Autopilot Case | 6061 – T6 Al. Alloy | 0.097 | 0.230 | 0.1380 |
| | Batteries Case | 6061 – T6 Al. Alloy | 0.097 | 0.230 | 0.1380 |
| | Inverter Case | 6061 – T6 Al. Alloy | 0.097 | 0.230 | 0.1380 |

## Table 2. Thermal Property Conversion Constants

A.  Density, $\rho$

$$1 \text{ lbm/in.}^3 = 0.00058 \text{ lbm/ft}^3$$
$$= 0.03609 \text{ gm/cm}^3$$

B.  Specific Heat, $C_p$

$$1 \text{ Btu/lbm-}°F = 1.00078 \text{ cal/gm-}°C$$

C.  Conductivity, k

$$1 \text{ Btu/in.-min-}°F = 0.00012 \frac{\text{Btu-in.}}{\text{hr-ft}^2\text{-}°F}$$
$$= 0.0014 \frac{\text{Btu}}{\text{hr-ft-}°F}$$
$$= 5 \frac{\text{Btu}}{\text{ft-sec-}°F}$$
$$= 0.336 \frac{\text{cal-cm}}{\text{cm}^2\text{-sec-}°C}$$
$$= 0.0802 \text{ watts/cm-}°C$$
$$= 0.000932 \text{ Kcal/m-hr-}°C$$

Table 3.  Bomb Section Rake Thermocouple Locations

| Rake No. | Bomb Station, in. | Thermocouple Identification | X/L | φ, deg | Thermocouple Location Measured from Asphalt Liner Plaster Interface, in. |
|---|---|---|---|---|---|
| 1 | 72.5 | TR11 | 0.487 | −10 | 0 |
| | | 12 | | | 0.25 |
| | | 13 | | | 0.50 |
| | | 14 | | | 1.00 |
| | | 15 | | | 1.50 |
| | | 16 | | | 2.00 |
| | | 17 | | | 2.50 |
| | | 18 | | | 3.00 |
| | | 19 | | 80 | 0 |
| | | 110 | | | 0.25 |
| | | 111 | | | 0.50 |
| | | 112 | | | 1.00 |
| | | 113 | | | 1.50 |
| | | 114 | | | 2.00 |
| | | 115 | | | 2.50 |
| | | 116 | | | 3.00 |
| | | 117 | | 170 | 0 |
| | | 118 | | | 0.25 |
| | | 119 | | | 0.50 |
| | | 120 | | | 1.00 |
| | | 121 | | | 1.50 |
| | | 122 | | | 2.00 |

Table 3.  Concluded

| Rake No. | Bomb Station, in. | Thermocouple Identification | X/L | φ, deg | Thermocouple Location Measured from Asphalt Liner Plaster Interface, in. |
|:---:|:---:|:---:|:---:|:---:|:---:|
| 1 | 72.5 | TR123 | 0.487 | 170 | 2.50 |
| ↓ | ↓ | 124 | ↓ | ↓ | 3.00 |
|  |  | 125 |  | 260 | 0 |
|  |  | 126 |  |  | 0.25 |
|  |  | 127 |  |  | 0.50 |
|  |  | 128 |  |  | 1.00 |
|  |  | 129 |  |  | 1.50 |
|  |  | 130 |  |  | 2.00 |
|  |  | 131 |  |  | 2.50 |
| ↓ | ↓ | 132 | ↓ | ↓ | 3.00 |
| 2 | 62.5 | TR21 | 0.419 | −10 | 0 |
| ↓ | ↓ | 22 | ↓ | 80 |  |
|  |  | 23 |  | 170 |  |
|  |  | 24 |  | 260 | ↓ |
|  |  | 25 |  | −10 | 1.00 |
|  |  | 26 |  | 80 |  |
|  |  | 27 |  | 170 |  |
|  |  | 28 |  | 260 | ↓ |
|  |  | 29 |  | −10 | 2.00 |
|  |  | 210 |  | 80 |  |
|  |  | 211 |  | 170 |  |
| ↓ | ↓ | 212 | ↓ | 260 | ↓ |

Table 4.  Component Time to Critical Temperature — Ground Test Summary

| Section | Component | Time to Critical Temperature, min |
|---------|-----------|-----------------------------------|
| Bomb | Asphalt/Plaster Interface<br>0.25 in. into Plaster<br>0.50 in. into Plaster | 7.5<br>25.0<br>45.5 |
| Guidance | Guidance Electronics Case<br>Printed Circuit Card<br>Stable Platform<br>Vidicon Tube | 33.0<br>38.0<br>>60.0 |
| Control | Inverter<br>Roll Gyro<br>Auto Pilot<br>Batteries | 48.0<br>>60.0 |

64

# NOMENCLATURE

$C_p$    Material specific heat at constant pressure, Btu/lbm-°F

GBxx    Bomb section heat flux gage identification, Fig. 17

GCxx    Control section heat flux gage identification, Fig. 20

GDxx    Guidance section heat flux gage identification, Fig. 19

$h$    Heat-transfer coefficient, $h = \dot{q}/(T_r - T_w)$, Btu/ft²-sec-°F

$k$    Material conductivity, Btu/in.-min-°F

$L$    Length of store, in.

$M_e$    Mach number at the edge of the boundary layer

$M_\infty$    Free-stream Mach number

$\dot{q}$    Heat-transfer rate, Btu/ft²-sec

$\dot{q}_i$    Heat-transfer rate at the beginning of each ground test run, Btu/ft²-sec

$r$    Recovery factor - a measure of the energy in a flow being brought to rest through viscous action

$\overline{T}$    Nondimensional temperature term defined by $\overline{T} = T_{(t)} - T_i/T_r - T_i$

TRxx    Bomb section rake thermocouple identification, Fig. 18.

$T_{crit}$    The temperature at which store component degradation or failure occurs as determined by the failure criteria, °F

$\overline{T}_{crit}$    Component critical temperature limit in nondimensional $\overline{T}$ form, $\overline{T}_{crit} = T_{crit} - T_i/T_r - T_i$, Fig. 29

$T_e$    Fluid temperature at the edge of the boundary layer, °F

$T_i$       Store component initial temperature, °F

$T_o$       Free-stream total temperature, °F

$T_r$       Recovery temperature or that temperature which the store would reach if flown at a given Mach number and altitude for an infinitely long period of time, °F

$T_{(t)}$       Component temperature at time t, °F

$T_w$       Store wall temperature, °F

$T_\infty$       Free-stream static temperature, °F

t       Time, min

$t_{crit}$       Time required for the store component to reach its critical temperature, min

X       Axial distance measured from the nose of the store to a particular instrumentation location, in.

$\varrho$       Material density, lbm/in.$^3$

$\phi$       Circumferential location of the bomb rake thermocouple legs, deg